The TSC-RHEB-mTORC1 signaling pathway forms a novel auto-regulatory feedback loop

Doctoral thesis

for

the award of the doctoral degree

of the Faculty of Mathematics and Natural Sciences

of the University of Cologne

submitted by

Andreas Lamprakis

accepted in the year 2026

Table of Contents

1 Introduction 12

1.1 Regulation of protein, nucleotide, and lipid biosynthesis by mTORC1 13

1.2 mRNA Translation 14

1.3 Repression of autophagy 14

1.4 De novo Nucleotide synthesis 15

1.5 Lipid biogenesis 15

1.6 Lysosome biogenesis 16

1.7 The mTOR Pathway (TSC-RHEB-mTORC1) 17

1.8 Growth factor signaling (PI3K-AKT & ERK-RSK pathways) 21

1.9 Amino acid signaling 23

1.10 Amino-acid sensors 24

1.11 Energy sensing 26

1.12 mTORC2 signaling and regulation 28

1.13 mTOR signaling in disease 29

1.14 mTOR feedback regulation 30

2 Aims 32

3 Results 34

3.1 RHEB activity drives TSC1 phosphorylation 34

3.2 mTORC1 mediates the effect of RHEB on TSC1 phosphorylation 35

3.3 TSC complex integrity is required for TSC1 phosphorylation 36

3.4 TSC1 is a novel substrate of mTORC1 39

3.5 TSC1 is a novel lysosomal substrate of mTORC1 41

3.6 Physiological stresses impinge on TSC1 phosphorylation 43

3.7 mTORC1 promotes TSC1 stability and binding to 14-3-3 anchor proteins 45

3.8 TSC1 phosphorylation regulates the lysosomal branch of mTORC1 signaling 48

4 Discussion 49

5 Future perspectives 55

5.1 Open questions based on the presented findings 55

5.2 mTORC1 and CDK1 signaling converge on TSC1 55

5.3 Resistance to cancer therapeutics 56

6 Materials and methods 59

6.1 Cell culture 59

6.2 Cell culture treatments 59

6.3 Generation of knockout cell lines 61

6.4 Generation of stable cell lines 61

6.5 Cell lysis and immunoblotting 62
6.6 Immunoprecipitation (co-IP/IP) 64
6.7 Sample preparation for mass-spectrometry 65
6.8 Gene silencing experiments 66
6.9 RNA isolation and cDNA synthesis 66
6.10 Plasmid transfections 66
6.11 Plasmids and molecular cloning 66
6.12 mTOR kinase activity assay 67
6.13 Recombinant protein expression 68
6.14 Statistical analysis 68

7 References 69

Abbreviations

mTOR	mechanistic target of Rapamycin
mTORC1	mTOR Complex 1
mTORC2	mTOR Complex 2
RAPTOR	regulatory-associated protein of mTOR
RICTOR	rapamycin-independent companion of mTOR
mSIN1	mammalian stress-activated protein kinase-interacting protein 1
PRAS40	proline-rich AKT substrate 40 kDa
mLST8	mammalian lethal with SEC13 protein 8
DEPTOR	DEP-domain-containing mTOR-interacting protein
TOS	TOR signaling motifs
HEAT	Huntingtin, EF3, PP2A, TOR1
FAT	FRAP, ATM, TRRAP
FRB	FKBP-Rapamycin-binding
4E-BP1	4E-binding protein 1
eIF4G	eukaryotic initiation factor 4G
eIF4E	eukaryotic initiation factor 4E
eIF4A	eukaryotic initiation factor 4A
eIF4B	eukaryotic initiation factor 4B
S6K1	p70 S6 Kinase 1
RPS6	ribosomal protein S6
RAS	rat sarcoma
RAF	rapidly accelerated fibrosarcoma
MEK	mitogen-activated protein kinase kinase
ERK1/2	extracellular signal-regulated kinases
RSK1/2	p90 ribosomal S6 kinases 1/2
S6	ribosomal protein S6
PDPK1	phosphoinositide-dependent protein kinase 1
FKBP12	FK506-binding protein 12
TOP	terminal oligopyrimidine tract
FIP200	200-kDa FAK family kinase-interacting protein

ULK1	serine/threonine-protein kinase ULK1
ATG13	autophagy-related protein 13
ATG14	autophagy-related protein 14
PI3K	phosphatidylinositol 3-kinase
PIK3CA	phosphatidylinositol 3-kinase catalytic subunit
PIP	phosphatidylinositol phosphate
PIP3	phosphatidylinositol (3,4,5)-trisphosphate
PIP2	phosphatidylinositol (4,5)-trisphosphate
TFEB	transcription factor EB
TFE3	transcription factor E3
CLEAR	coordinated lysosomal expression and regulation
RHEB	Ras-homolog enriched in brain
Rags	Ras-related GTP-binding proteins
TSC	tuberous sclerosis complex
TSC1	tuberous sclerosis complex 1
TSC2	tuberous sclerosis complex 2
TBC1D7	TBC1 domain family member 7
GEF	guanine exchange factors
GAP	GTPase-activating protein domain
GTP	guanosine triphosphate
GDP	guanosine diphosphate
PKB/AKT	protein kinase B
FOXO	forkhead box proteins
SGK1	serine/threonine-protein kinase SGK1
PH	pleckstrin-homology
PTEN	phosphatidylinositol 3,4,5-trisphosphate 3-phosphatase and dual-specificity protein phosphatase PTEN
TSC	tuberous sclerosis
LOH	loss-of-heterozygosity
G3BPs	Ras GTPase-activating protein-binding proteins
IRS1/2	insulin receptor substrate 1/2
GRB10	growth factor receptor-bound protein 10

CDK1	cyclin-dependent kinase 1
AMPK	5'-AMP-activated protein kinase
GATOR1	GAP activity towards Rags 1
GATOR2	GAP activity towards Rags 2
SLC38A9	sodium-coupled neutral amino acid transporter 9
DEPDC5	DEP domain-containing 5
NPRL2	nitrogen permease regulator-like 2
NPRL3	nitrogen permease regulator-like 3
MIOS	meiosis regulator for oocyte development
WDR24	WD repeat domain 24
WDR59	WD repeat domain 59
SEH1L	seh1 like nucleoporin
SEC13	sec13 homolog nuclear pore and COPII coat complex component
KPTN	Kaptin
ITFG2	integrin-α FG-GAP repeat containing 2
SZT2	C12orf66 and seizure threshold 2
FLCN	folliculin
FNIP1/2	FLCN-interacting proteins 1 and 2
CASTOR1/2	cytosolic arginine sensor for mTORC1
KO	knockout
WT	wild-type
HEK	human embryonic kidney
MEFs	murine embryonic fibroblasts
IVK	*in vitro* kinase assay
siRNAs	small interfering RNAs
HA	hemagglutinin
GF	growth factors
AA	amino acids
GAPDH	glyceraldehyde-3-phosphate dehydrogenase
DMEM	Dulbecco's modified eagle medium
FBS	fetal bovine serum

P/S	penicillin-streptomycin
PCR	polymerase chain reaction
dFBS	dialyzed FBS
cDNA	complementary DNA
RT-qPCR	reverse transcription quantitative real-time PCR
SDS-PAGE	sodium dodecyl sulphate polyacrylamide gel electrophoresis
BSA	bovine serum albumin
NaF	sodium fluoride
DTT	dithiothreitol
PP	protein phosphatase
IPTG	isopropyl-β-D-thiogalactopyranoside
SD	standard deviation

Abstract

The mechanistic target of rapamycin complex 1 (mTORC1) regulates cell growth and metabolism by integrating a wide range of intracellular and extracellular cues. Many kinases signal the availability of these inputs through phosphorylation events on the TSC complex, the major negative regulator in the mTOR pathway. Because of the involvement of mTORC1 in a multitude of biological processes, cells have evolved feedback loops to tightly regulate the activity of the pathway. Upon sustained mTORC1 inhibition, compensatory activation of signaling branches upstream of the TSC complex restores basal mTORC1 activity to maintain essential cellular functions. However, the signaling events involved in mTORC1 auto-regulation are not fully understood. Here, I find that TSC1, a component of the TSC complex, is a novel lysosomal substrate of mTORC1. TSC1 phosphorylation on mTORC1-dependent sites promotes its stability and binding to 14-3-3 anchor proteins. In a phospho-deficient mutant, TSC1 protein levels and the binding affinity to 14-3-3s decrease. Despite the general role of the TSC complex in regulating mTORC1 activity, TSC1 phosphorylation specifically regulates the lysosomal branch of mTORC1 signaling. Hypophosphorylated TSC1 is associated with lower levels of TFEB phosphorylation, while the phosphorylation status of the non-lysosomal substrates, such as S6K1, remains largely unaffected. Based on these findings, my work sheds light on the shortest feedback loop in the mTOR pathway providing a deeper understanding of the mechanistic underpinnings of mTORC1 auto-regulation with implications on the phosphorylation of substrates involved in catabolic processes.

Zusammenfassung

Der mechanistische Zielkomplex des Rapamycins 1 (mTORC1) reguliert Zellwachstum und Stoffwechsel, indem er eine Vielzahl intra- und extrazellulärer Signale integriert. Viele Kinasen vermitteln die Verfügbarkeit dieser Inputs über Phosphorylierungsereignisse am TSC-Komplex, dem wichtigsten negativen Regulator im mTOR-Signalweg. Aufgrund der Beteiligung von mTORC1 an zahlreichen biologischen Prozessen haben Zellen Rückkopplungsschleifen entwickelt, um die Aktivität des Signalwegs streng zu kontrollieren. Bei anhaltender mTORC1-Hemmung führt eine kompensatorische Aktivierung von Signalzweigen stromaufwärts des TSC-Komplexes zur Wiederherstellung der basalen mTORC1-Aktivität, um essenzielle zelluläre Funktionen aufrechtzuerhalten. Die an der Autoregulation von mTORC1 beteiligten Signalereignisse sind jedoch nicht vollständig verstanden. Hier zeige ich, dass TSC1, eine Komponente des TSC-Komplexes, ein neuartiges lysosomales Substrat von mTORC1 ist. Die Phosphorylierung von TSC1 an mTORC1-abhängigen Stellen fördert seine Stabilität und die Bindung an 14-3-3-Ankerproteine. In einem phospho-defizienten Mutanten sinken sowohl die TSC1-Proteinspiegel als auch die Bindungsaffinität zu 14-3-3-Proteinen. Trotz der allgemeinen Rolle des TSC-Komplexes bei der Regulation der mTORC1-Aktivität steuert die Phosphorylierung von TSC1 spezifisch den lysosomalen Zweig der mTORC1-Signalgebung. Hypophosphoryliertes TSC1 ist mit niedrigeren TFEB-Phosphorylierungsniveaus assoziiert, während der Phosphorylierungsstatus nicht-lysosomaler Substrate wie S6K1 weitgehend unbeeinflusst bleibt. Auf Basis dieser Befunde beleuchtet meine Arbeit die kürzeste Rückkopplungsschleife im mTOR-Signalweg und ermöglicht ein tieferes Verständnis der mechanistischen Grundlagen der mTORC1-Autoregulation – mit Implikationen für die Phosphorylierung von Substraten, die an katabolen Prozessen beteiligt sind.

List of Figures

Figure 1.1. Structural and domain organization of mTORC1 and mTORC2. 13
Figure 1.2. Insights into the structure of TSC complex assembly and its GAP activity on RHEB. 19
Figure 1.3. Cryo-EM derived structure of human mTORC1. 20
Figure 1.4. mTORC1 signal integration by the RAS-ERK and PI3K-AKT pathways. 23
Figure 1.5. mTORC1 lysosomal amino acid sensing machinery. 26
Figure 1.6. AMPK-mediated phosphorylation events inhibit mTORC1 signaling. 28
Figure 1.7. Feedback inhibition downstream of mTORC1. 30
Figure 3.1. RHEB activity causes TSC1 phosphorylation. 34
Figure 3.2. mTORC1 mediates TSC1 phosphorylation in response to RHEB activity. 35
Figure 3.3. TSC2 loss abrogates TSC1 phosphorylation in cells with hyperactive mTORC1. 36
Figure 3.4. Upregulation of the mTOR pathway drives TSC1 phosphorylation. 37
Figure 3.5. mTORC1 hyperactivity causes an increase in TSC1 phosphorylation on S1080. 38
Figure 3.6. mTOR phosphorylates TSC1 in vitro. 39
Figure 3.7. mTORC1 interacts with the TSC complex. 40
Figure 3.8. TSC complex integrity is dispensable for binding to mTORC1. 41
Figure 3.9. The lysosomal mTORC1 machinery is required for mTORC1 signaling to TSC1. 42
Figure 3.10. Lysosomal tethering of the TSC complex is necessary for TSC1 phosphorylation. 43
Figure 3.11. mTORC1 inhibition in response to physiological stresses diminishes TSC1 phosphorylation. 44
Figure 3.12. TSC1 dephosphorylation kinetics in response to pharmacological mTORC1 inhibition. 45
Figure 3.13. TSC1 phosphorylation promotes its stability. 46
Figure 3.14. Decreased TSC1 protein stability is not due to weaker binding to TSC2. 46
Figure 3.15. TSC1 phosphorylation promotes the binding of 14-3-3 anchor proteins to the TSC complex. 47
Figure 3.16. Recovery in TFEB phosphorylation is blunted in the TSC1-2A deficient mutant. 48
Figure 4.1. TSC1 phosphorylation on mTORC1-dependent sites promotes its stability and binding to 14-3-3 anchor proteins. 52

List of Tables

Table 1. Inorganic components and amino acids used for the preparation of custom-made media. 60
Table 2. Oligonucleotide sequence of single-guide RNAs. 61
Table 3. Antibodies used in co-IP/IP, Western blot, and IVK assay experiments. 63
Table 5. Mutagenic oligonucleotide sequences used in molecular cloning. 67

1 Introduction

Rapamycin, originally identified in the 1960s and subsequently isolated from *Streptomyces hygroscopicus* by Suren Sehgal, is an extraordinary pharmacological compound renowned for its potent antifungal, immunosuppressive, and cytostatic anticancer properties [1]. The intricate mechanisms through which Rapamycin exerts its diverse cellular effects remained an enigma until the early 1990s when a group of scientists at the University of Basel in Switzerland defined the TOR genes (target of Rapamycin) by characterizing drug-resistant yeast mutants [2]. Soon after, the discovery of the yeast TOR proteins came along, followed by the identification, purification, and cloning of their mammalian counterparts (mTOR) [3-7]. These discoveries paved the way for intensive exploratory efforts in the following decades that led to our current understanding of mTOR as a master regulator of growth and metabolism.

mTOR operates as a part of two similarly organized but functionally distinct protein complexes. In mammalian cells, the rapamycin-sensitive mTOR complex 1 (mTORC1) promotes protein, nucleotide, and lipid synthesis and inhibits autophagy and lysosome biogenesis; in contrast, the partially rapamycin-insensitive mTOR complex 2 (mTORC2) governs processes related to cytoskeletal organization, cell survival, and proliferation (Figure 1.1) [8]. Rapamycin inhibits mTORC1 by forming a gain-of-function complex with the cytoplasmic immunophilin FKBP12 (FK506-binding protein of 12 KDa) [9]. FKBP12-Rapamycin does not induce a conformational change in mTOR but instead binds the FRB domain at the lip of the mTOR catalytic cleft, forming a lid that physically prevents access of substrates to the catalytic site [10-12]. In addition to a difference in sensitivity to Rapamycin, in both yeast and metazoans, either complex contains unique accessory components including, but not restricted to, regulatory associated protein of mTOR (RAPTOR) in mTORC1, and mSIN1 (mammalian stress-activated protein kinase-interacting protein 1) and rapamycin-independent companion of mTOR (RICTOR) in mTORC2 (see Fig.1 for more details). RAPTOR is essential for proper subcellular localization of mTORC1 and substrate recruitment through the TOR signaling (TOS) motifs that are present on several known canonical targets [10, 13-15]. mSIN1 mediates mTORC2 recruitment to the plasma

membrane by way of its phospholipid-binding pleckstrin homology (PH) domain, whereupon it carries out its catalytic activity toward downstream effectors [8]. The functional role of RICTOR has yet to be elucidated. However, structural evidence indicates that its orientation relative to mTORC2 occludes Rapamycin from binding and inhibiting the complex. Notably, in a number of cell lines, prolonged exposure to Rapamycin impedes mTORC2 assembly by preventing mTOR nucleation into nascent complexes [16].

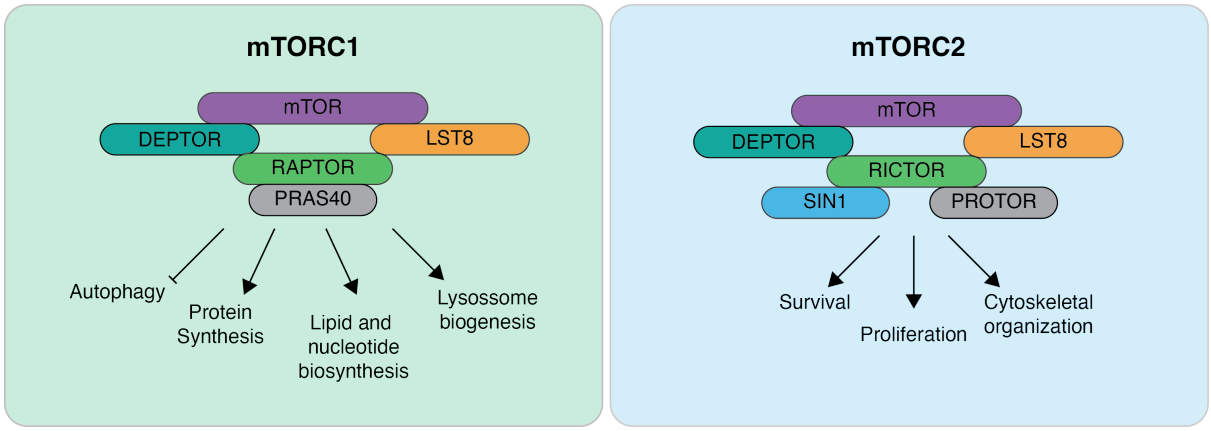

Figure 1.1. Structural and domain organization of mTORC1 and mTORC2.
mTORC1 and mTORC2 are composed of shared and unique components. Both contain mTOR, DEP domain containing mTOR interacting protein (DEPTOR), and mammalian lethal with SEC13 protein 8 (mLST8). RAPTOR and proline-rich AKT substrate of 40 kDa (PRAS40) are unique to mTORC1, whereas RICTOR, mSIN1, and protein observed with RICTOR (PROTOR) are unique to mTORC2. The two complexes exhibit distinct functions within the cell. mTORC1 primarily integrates signals related to nutrient availability to balance anabolic and catabolic processes. In contrast, mTORC2 regulates cytoskeletal dynamics and activates various pro-survival signaling pathways. Notably, while mTORC1 is acutely inhibited by Rapamycin, mTORC2 is only affected by prolonged Rapamycin treatment. Adapted from Liu & Sabatini and Goul *et al.* [8, 17].

1.1 Regulation of protein, nucleotide, and lipid biosynthesis by mTORC1

mTORC1 activation leads to numerous metabolic changes ultimately aimed to switch the cell into an anabolic growth state that supports accumulation of biomass. These changes occur through mTORC1-mediated phosphorylation and activation of numerous positive regulators of anabolic programs, of which ribosomal protein S6 kinase B1 and B2 (S6K1 and S6K2) stand prominent, and through phosphorylation and inactivation of negative regulators including eukaryotic translation initiation factor 4E-binding protein 1 and 2 (4E-BP1 and 4E-BP2), transcription factor EB (TFEB) and TFE3, and the autophagy-related proteins, unc-51-like autophagy-activating kinase 1 (ULK1) and autophagy-related protein 13 (ATG13).

1.2 mRNA Translation

There are two S6Ks in mammals, encoded by separate genes, of which S6K1 is the best characterized. S6K1 activation requires the phosphorylation of two essential residues namely T229 by PDPK1, which is located in the catalytic activation loop, and T389 by mTORC1, found in the hydrophobic motif. Many of the eukaryotic translation initiation factors (eIF), which are part of the eIF4F RNA helicase complex are targets of S6K1 [18]. In particular, the initiation factor eIF4A possesses RNA helicase activity and unwinds structured mRNAs during translation initiation in an ATP-dependent manner. Although eIF4A alone exhibits low levels of RNA helicase activity, its function is substantially increased by eIF4B. S6K1 phosphorylation on S422 of eIF4B promotes its incorporation into the translation pre-initiation complex whereupon it enhances the ATP processivity of eIF4A [19-21]. S6K1 also phosphorylates Programmed cell death (PDCD4) on S67, which results in its ubiquitination and subsequent degradation through the E3 ubiquitin ligase βTrCP [22]. When S6K1 activity is suppressed, PDCD4 competes with eIF4A for binding to the eIF4F complex inhibiting the translation of mRNAs with structured 5' untranslated region (UTR) [23, 24]. mTORC1 also regulates cap-dependent translation initiation through direct phosphorylation of 4E-BP1 on T37, T46, S65, T70, and S83. Hypophosphorylated 4E-BP1 associates with eIF4E that binds to the 5' mRNA 7-methyguanosine cap occluding access to the eIF4F structure. mTORC1 activity promotes the displacement of 4E-BP1 and efficient recruitment of eIF4E to the 5' end of mRNA [25-27]. Lastly, another substrate of mTORC1, the RNA-binding protein La-related protein 1 (LARP1) appears to directly bind 5′ terminal oligo-pyrimidine tract motif (TOP) sequences and repress mRNA translation. The mTORC1-mediated phosphorylation of LARP1 causes it to dissociate from the 5′ UTR, thus allowing for the recruitment of eIF4G scaffold protein and the formation of a functional eIF4F complex [28, 29].

1.3 Repression of autophagy

When nutrients are available, active mTORC1 phosphorylates and inhibits multiple autophagy-regulating proteins to prevent a futile cycle in which newly synthesized cellular components are prematurely broken down. To that end, mTORC1 applies inhibitory phosphorylation marks to unc-51-like autophagy-activating kinase 1 (ULK1)

and autophagy-related protein 13 (ATG13), which together with FAK family kinase-interacting protein of 200 kDa (FIP200) and ATG101 form the ULK complex, blocking autophagosome biogenesis and initiation of autophagy [30-32]. In addition, mTORC1 phosphorylates autophagy factors that are important for the nucleation stage of autophagy, such as ATG14, thereby inhibiting the ATG14-containing PI3K-III complex and nuclear receptor binding factor 2 (NRBF2), a regulator of the PI3K-III complex [33, 34].

1.4 *De novo* Nucleotide synthesis

To maintain DNA replication mTORC1 stimulates the *de novo* synthesis of both pyrimidine and purine nucleotides. Recent work has shown that mTORC1 activates the transcription factor ATF4 and its downstream target, mitochondrial tetrahydrofolate cycle enzyme methylenetetrahydrofolate dehydrogenase 2 (MTHFD2) [35]. MTHFD2 drives *de novo* purine synthesis via the formation of N10-formyltetrahydrofolate, a cofactor required for the purine synthesis enzymes phosphoribosylglycinamide formyltransferase (GART) and inosine monophosphate synthase (ATIC) [36]. In addition, activation of mTORC1 acutely stimulates an increased flux through the *de novo* pyrimidine-synthesis pathway via S6K1-mediated phosphorylation of the rate-limiting enzyme carbamoyl-phosphate synthase 2, aspartate transcarbamylase, dihydroorotase (CAD) [36, 37]. CAD catalyzes the first three steps in *de novo* pyrimidine synthesis, and CAD phosphorylation by S6K1 on S1859 is required for the production of new nucleotides to accommodate an increase in DNA synthesis during anabolic growth [38].

1.5 Lipid biogenesis

As cells increase in size, they must generate lipids to sustain biogenesis of new membranes. Accordingly, mTORC1 drives lipid synthesis through activation of the sterol regulatory element binding protein 1 and 2 (SREBP1 and 2) family of transcription factors. Sterol depletion triggers the translocation of SREBPs to the Golgi apparatus where they undergo proteolytic cleavage such that an active amino-terminal fragment is released. The mature active form of SREBPs enters the nucleus and binds sterol regulatory elements in the promoters of target genes inducing their expression

[39]. mTORC1 activates the SREBP transcriptional program by phosphorylating LIPIN1 [40]. Hyper-phosphorylated LIPIN1 is sequestered in the cytoplasm promoting SREBP processing and nuclear localization. Although the mechanism remains unclear, mTORC1 may also enhance the nuclear translocation and processing of the SREBPs in an S6K1-dependent manner [38, 41].

1.6 Lysosome biogenesis

TFEB acts as a master regulator of lysosomal biogenesis by coordinating the transcriptional upregulation of lysosomal membrane proteins and lysosomal hydrolases. Together with TFE3, TFEC, and MITF, it belongs to the microphthalmia/transcription factor E (MiT/TFE) family of basic helix–loop–helix leucine zipper (bHLH-Zip) transcription factors [42]. TFEB forms a homodimer or heterodimer with other MiT/TFE members and has an affinity for an asymmetric E-box-like 10 base-pair (bp) motif (5'-GTCACGTGAC-3'), termed the "coordinated lysosomal expression and regulation (CLEAR)" element, found within 200 bp of the transcription start site in the promoters of the target genes [43]. TFEB sub-cellular localization, and hence the capacity to exert its biological role, is heavily regulated by the presence of post-translational modifications [43]. The main kinase that determines whether TFEB resides at rest in the cytosol, or whether it can bind CLEAR motifs within promoters of target genes in the nucleus, is mTORC1. Active mTORC1 directly phosphorylates TFEB on three crucial residues — S122, S142, and S211 — thereby facilitating its binding to 14-3-3 proteins and its retention in the cytoplasm [44-48]. TFEB together with TFE3 are the first substrates to be reported where the lysosomal nutrient sensing machinery of mTORC1 is actively involved in their recruitment to the lysosome to be phosphorylated [49-52]. Indeed, recent structural analysis of an mTORC1 megacomplex encompassing TFEB, RagA-C, and the LAMTOR complex revealed the presence of extensive contact sites between TFEB and $RagC^{GDP}$ [53]. Intriguingly, contrary to the other mTORC1 targets, TFEB and TFE3 phosphorylation is not abolished when growth factors are absent. Even more paradoxical is the fact that mTORC1 hyper-activation in cells lacking TSC1 or TSC2 does not correlate with elevated TFEB phosphorylation despite an overt increase in the phosphorylation of common readouts of mTORC1 activity, such as 4E-BP1 and S6K1 [54]. As such,

TFEB and TFE3 are regarded as unconventional mTORC1 substrates, although mTORC1 inhibition in response to amino acid or glucose deprivation does elicit TFEB and TFE3 dephosphorylation.

1.7 The mTOR Pathway (TSC-RHEB-mTORC1)

The heterotrimeric TSC complex is the major negative regulator in the mTOR pathway that comprises the proteins TSC1, TSC2 (also known as Hamartin and Tuberin, respectively), and the auxiliary component TBC1D7 (TBC1 domain family member 7) in a 2:2:1 molar stoichiometry [55, 56]. Mutations in either *TSC1* or *TSC2* genes cause the autosomal dominant disorder Tuberous Sclerosis (TSC) characterized by the development of benign tumors (hamartomas) in the skin, liver, kidney, brain, lung, and heart [57]. TSC1 and TSC2 carry limited similarity to other proteins and are conserved in most eukaryotes, including fungi, with *S. cerevisiae* and *C. elegans* being some notable exceptions. TSC1 and TSC2 have been reported to form oligomeric structures in cells, but the functional significance of oligomerization has not been explored [58]. The N-terminal region of TSC2 consists of a HEAT repeat domain and is sufficient to mediate the interaction with TSC1, while the C-terminal TSC1 helical coiled-coil domain associates with TSC2 and TBC1D7 [59-61]. The TSC2 subunit contains a catalytic asparagine thumb at position 1643 embedded in the C-terminal GTPase-activating protein (GAP) domain (amino acids 1,538 – 1,729 in human TSC2) that is responsible for GTP hydrolysis (Figure 1.2) [62, 63]. However, TSC2 by itself is not functional *in vivo* and requires TSC1 as an obligate regulatory complex partner. TSC1 promotes TSC complex activity by stabilizing TSC2. Cells lacking TSC1 exhibit lower TSC2 protein levels owing to ubiquitination and proteasome-mediated degradation in response HERC1 E3 ligase activity [64]. Furthermore, TSC1 was reported to function as a co-chaperone for HSP90 for which TSC2 is a client protein, suggesting that TSC1 also stabilizes TSC2 by promoting proper folding [65]. More recently TSC1 was shown to be a determining factor in the proper sub-cellular localization of the complex. As such, the N-terminal domain in TSC1, composed of a wide basic surface was shown to confer specificity to phosphatidylinositol phosphate (PIP) species and mediate recruitment of the TSC complex to the lysosomal membrane, thus, ascribing a new functional role to TSC1 in TSC complex regulation [59]. Interestingly, although Tsc1

or Tsc2 KO mouse models are embryonically lethal, Tbc1d7 KO mice undergo normal growth and development, suggesting that TBC1D7 is a non-essential component of the complex during embryogenesis. In cultured cells, TBC1D7 gene silencing results in modest growth-factor-independent activation of mTORC1, albeit substantially less than that observed with loss of TSC1 or TSC2 owing to a partial destabilization of the TSC complex [66]. However, the effect on TSC complex integrity is only transient since TSC1 and TSC2 protein levels remain unchanged upon persistent loss of TBC1D7 [66]. Lysosomal recruitment of the TSC complex is integral to its ability in suppressing mTORC1 signaling [67, 68].

On lysosomes, the TSC complex interacts with the small GTPase Ras Homolog Enriched in Brain (RHEB) [62, 69, 70]. As with all GTPases, the nucleotide binding state of RHEB dictates the conformation of the switch I and switch II domains [71]. Only when bound to GTP, RHEB stabilizes the interaction between the TSC2 GAP and switch domains thereby promoting GTP hydrolysis [55]. GTPases possess a conserved glutamine residue that conveys intrinsic GTP hydrolysis activity. The conserved switch II Q64 residue in RHEB (equivalent to Q61 of RAS) is sterically hindered by being deeply embedded in a hydrophobic pocket and does not contribute to GTP hydrolysis, neither intrinsic nor GAP-stimulated [55]. As a result, RHEB exhibits low levels of intrinsic GTPase activity and is reported to exist primarily in its active GTP-bound state [71]. RHEB consists of 184 amino acid residues; the 169 N-terminal residues form the GTPase domain, while the 15 C-terminal residues comprise a hypervariable region with a conserved CAAX motif that plays an important role in RHEB farnesylation and endomembrane tethering [71]. Failure to localize to endomembranes impairs RHEB ability to interact with mTORC1 and activate downstream targets [72]. Despite the fact that RHEB has been shown to regulate mTORC1 activity on the Golgi, the conventional model describes mTORC1 activation by RHEB on the lysosomal surface [68, 73, 74]. Notably, RHEB was shown previously to reside on the endoplasmic reticulum (ER) and mitochondria but its effects on these other compartments were mTORC1-independent [75-78].

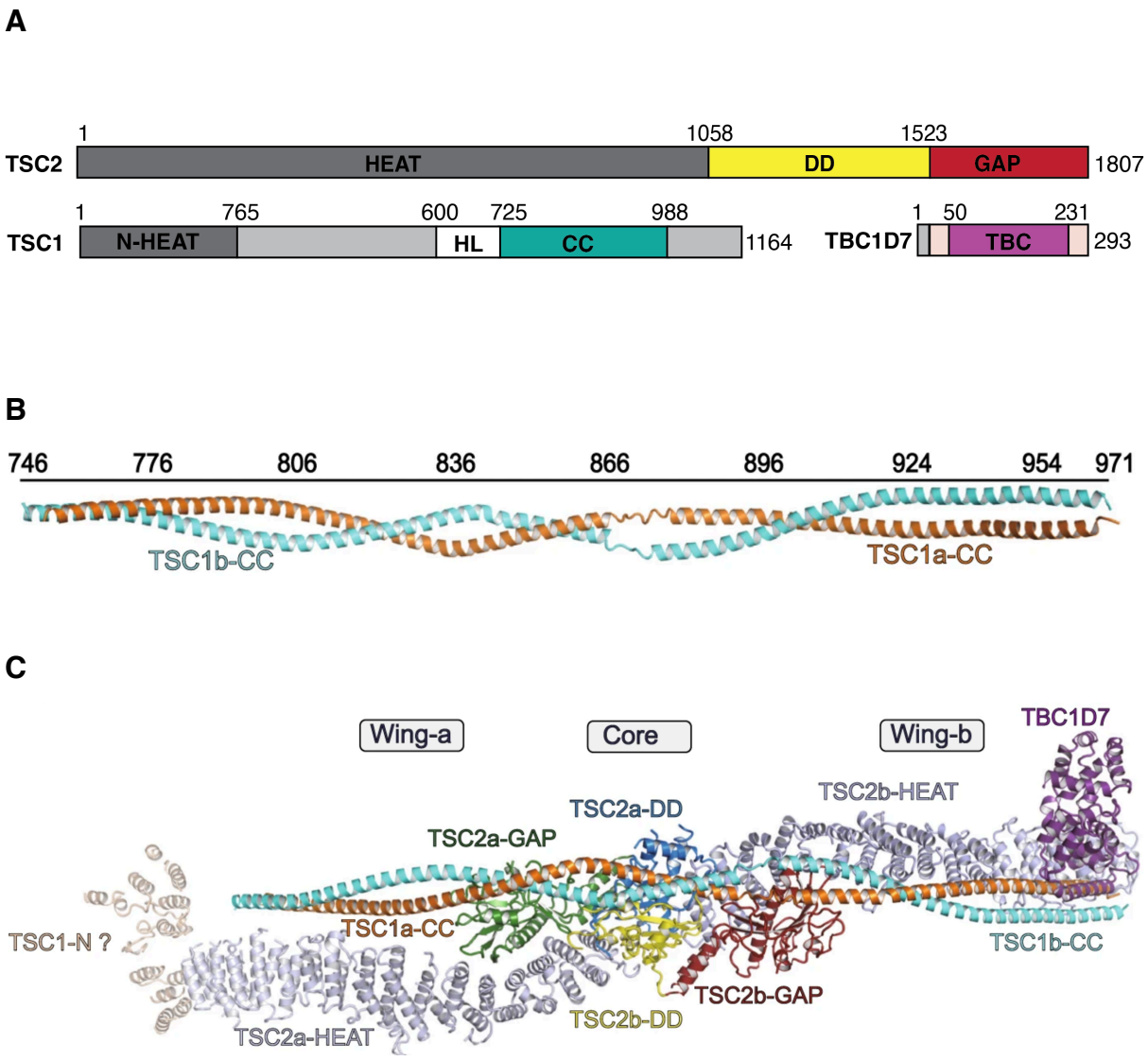

Figure 1.2. Insights into the structure of TSC complex assembly and its GAP activity on RHEB.
(A) Linear schematic of the TSC1, TSC2, and TBC1D7 domains. Colors correspond to the domains in the higher-order structures depicted in B and C.
(B) The coiled-coil domains of two TSC1 molecules are paired in parallel and form a two-turn left-handed supercoil. The TSC1 homodimer interface is enriched in nonpolar residues, which make extensive hydrophobic contacts to support a stable TSC1 dimerization and its scaffolding function. This parallel dimerization of TSC1 leads to an asymmetric formation of TSC1–TSC2 tetramer and recruitment of a single TBC1D7 molecule depicted in (C) [56].

When conditions are permissive, $RHEB^{GTP}$ binds to the N-terminal portions of the N-heat, M-heat, and FAT domains of mTOR, forming a four-way interface. Most of the contacts are made by the RHEB switch I (residues 33–41) and switch II (residues 63–79) regions [71]. Switch I binds to M-heat and FAT, whereas the longer switch II interacts with all three mTOR regions. RHEB activates mTORC1 by allosterically realigning the catalytic cleft bringing ATP-contacting residues in the N-lobe into close

proximity with critical C-lobe residues that include the Mg^{2+} ligands and two catalytic residues (Figure 1.3) [77, 78].

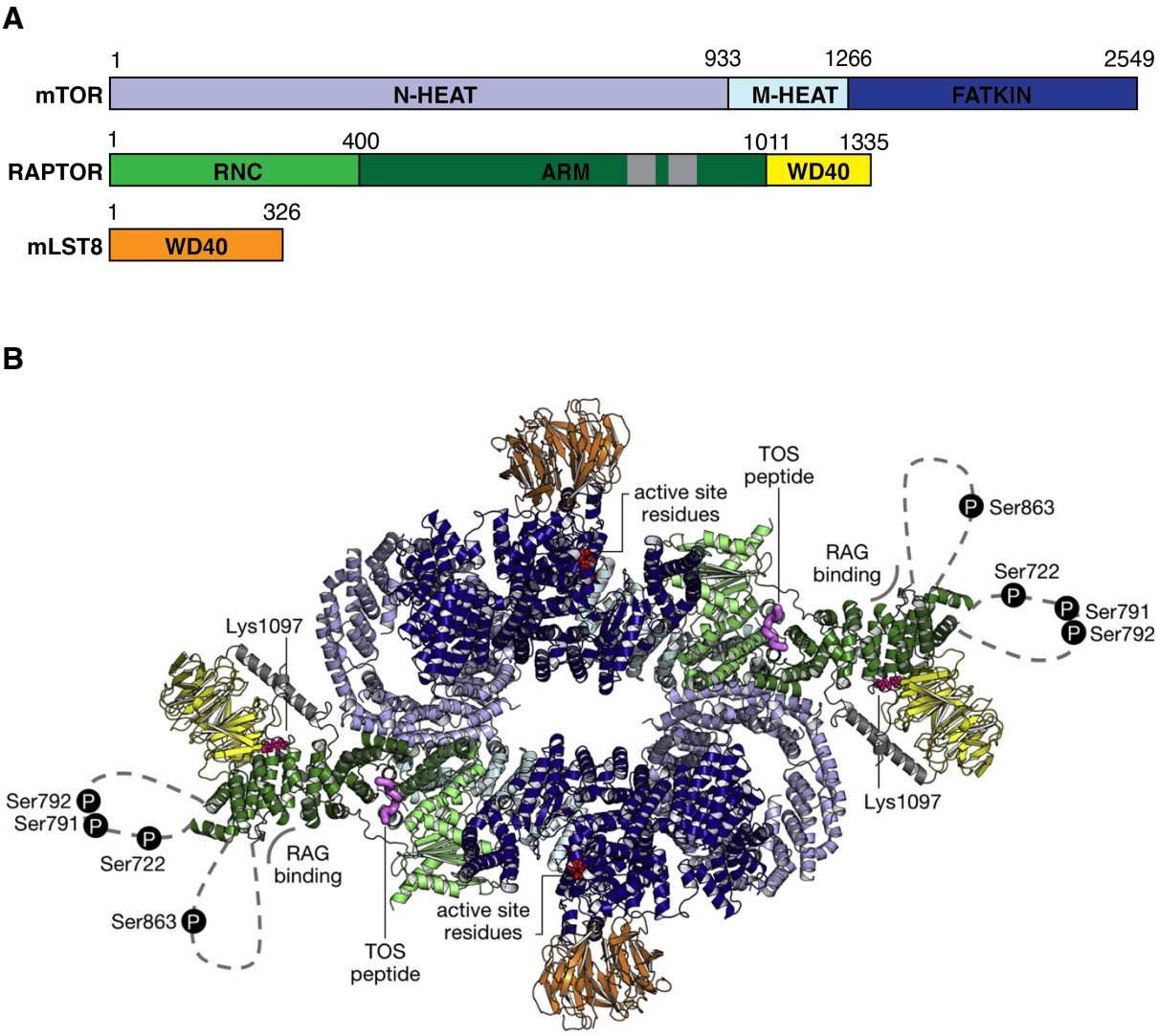

Figure 1.3. Cryo-EM derived structure of human mTORC1.
(A) Linear schematic of the domain organization of mTOR, RAPTOR, and mLST8. Color scheme corresponds to color-coded domains in the higher order structure depicted in (B).
(B) Model is based on available structural data by Yang *et al.* [12]. Domains are highlighted according to the primary structure scheme in (A). mTORC1 is a 1 MDa homodimer of heterotrimers (each of the latter containing mTOR, RAPTOR, and mLST8) that adopts a lozenge shape with a large central cavity. The two FATKIN regions come close to each other but make little or no contact. Each kinase site is located at the bottom of a deep catalytic cleft that is partly obstructed by neighboring structural elements, suggesting that the kinase activity is regulated by sterically restricting access to the catalytic cleft. The N- and M-HEAT repeats play an essential role in mTORC1 dimer formation, in which the N-HEAT domain of one copy of mTOR stacks against the M-HEAT of the other. The mTORC1 dimer interphase is probably conserved across orthologs due to the high degree of conservation in the HEAT region. RAPTOR further supports mTORC1 super-complex architecture whereby the ARM domain of one RAPTOR molecule locks onto the N-HEAT of one mTOR subunit and the M-HEAT of the other, thus stabilizing the two copies of mTOR. Adapted from Gonzalez *et al.* [79].

1.8 Growth factor signaling (PI3K-AKT & ERK-RSK pathways)

Binding of insulin and insulin-like growth factor 1 (IGF-1) to the insulin receptor that possesses receptor tyrosine kinase (RTK) activity, instigates a series of cross-phosphorylation events on tyrosine residues that are recognized by the adaptor proteins insulin receptor substrate 1 and 2 (IRS1/2) [36]. IRS1/2 scaffolds the recruitment of phosphatidylinositol 3-kinase (PI3K) promoting the formation of phosphatidylinositol 3,4,5-trisphosphate species on the plasma membrane that act as docking sites for the pleckstrin homology domain in AKT and 3-phosphoinositide dependent protein kinase 1 (PDPK1) [36]. While in vicinity, PDPK1 phosphorylates AKT on T308 in the activation loop stimulating its catalytic activity [36]. Notably, AKT phosphorylation on S473 in the hydrophobic motif by mTORC2 is not necessary for AKT activation but has been demonstrated to boost AKT activity particularly toward a subset of AKT substrates such as FOXO1/3$^{\alpha}$/4 [80]. Active AKT phosphorylates TSC2 on a number of residues including S939, S981, and T1462 [81]. These sites are recognized by 14-3-3 anchor proteins and are proposed to retain TSC away from the lysosome impeding TSC2 GAP activity toward RHEB [68, 82]. Importantly, TSC is not the only target of AKT in the mTOR pathway. 40 kDa Pro-rich AKT substrate (PRAS40) is an interactor and direct inhibitor of mTORC1 that blocks recruitment and proper alignment of the mTOR substrates to the active site [12, 83, 84]. Similar to that of TSC2, PRAS40 phosphorylation by AKT at T246 causes the binding of 14-3-3 proteins resulting in the dissociation of PRAS40 from mTORC1 [83]. The relative contributions of growth factor-mediated regulation of TSC–RHEB and PRAS40 downstream of AKT, and the importance of each branch in different cellular contexts remains an area of active study [17].

In parallel with the PI3K-AKT pathway, the mitogen-activated RAS-ERK signaling axis has also been shown to trigger the activation of mTORC1 signaling [85]. The agonists involved in RAS-ERK activation only partially overlap with those that signal to PI3K-AKT. PMA (phorbol 12-myristate 13-acetate) is generally a strong activator of the RAS-ERK pathway. By contrast, insulin, and IGF-1 are weaker RAS-ERK activators, but strong PI3K-AKT activators. Engagement of RTK and G protein-coupled receptors (GPCR) with their cognate ligands triggers the binding of SHC-transforming protein 1

(SHC) and growth factor receptor-bound protein 2 (GRB2) adaptor molecules to the cytoplasmic domain of the receptor. The presence of GRB2 at the plasma membrane generates binding sites for the guanine nucleotide exchange factor (GEF) son of sevenless (SOS), which catalyzes the conversion of RAS-GTPase to its active GTP-bound state. RAS engagement on the membrane increases the phosphorylation of the RAF kinase domain. Activated RAF kinase phosphorylates target proteins, such as MEK1 and MEK2, leading to the subsequent activation of extracellular signal-regulated kinases 1 and 2 (ERK1 and ERK2) and the end-point effectors ribosomal S6 kinase 1 and 2 (RSK1 and RSK2).

The RAS-ERK pathway engages in cross-activation of the PI3K-AKT and mTOR signaling cascades. Ras-GTP can directly bind to and allosterically activate PI3K [86-88]. Moreover, robust activation of the RAS-ERK pathway can enhance mTORC1 activity via ERK and RSK signaling directed at TSC2, exemplifying a sophisticated mechanism of signal integration. The ERK and RSK sites on TSC2 are different from those phosphorylated by AKT but function synergistically to inhibit TSC2 GAP function and promote mTORC1 activity [89, 90]. Lastly, although the underlying molecular mechanism is not fully defined, ERK and RSK can directly target mTORC1 by phosphorylating RAPTOR and thereby promote mTORC1 kinase activity [91]. Together, these findings suggest that the mitogen-activated RAS–ERK–RSK signaling module, in parallel with the PI3K–AKT pathway, contains several inputs to stimulate mTORC1 signaling (Figure 1.4) [85].

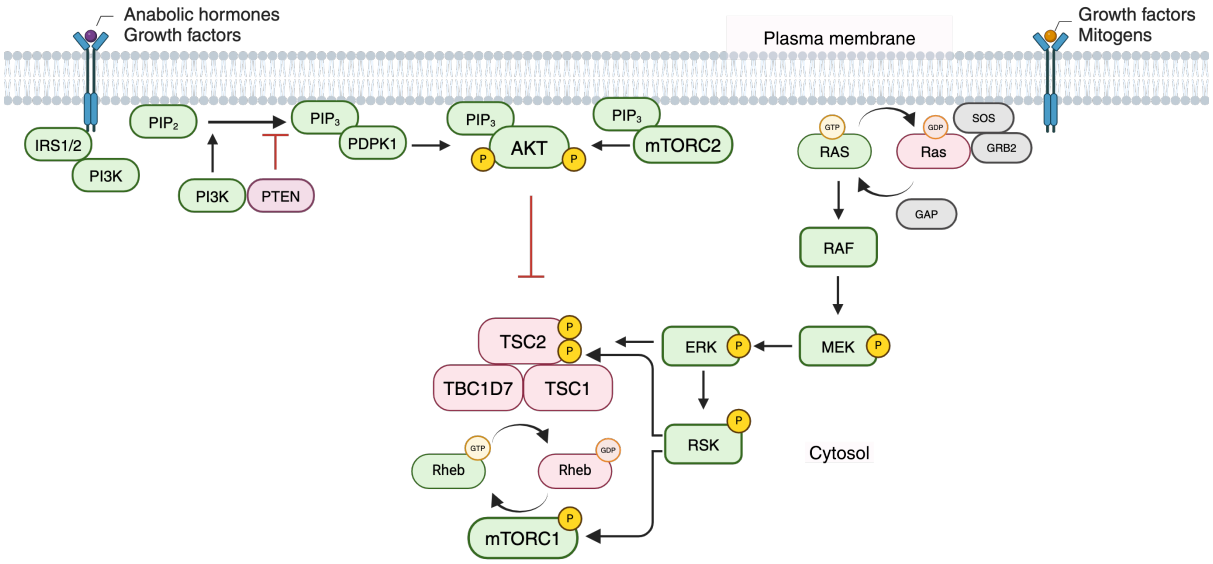

Figure 1.4. mTORC1 signal integration by the RAS-ERK and PI3K-AKT pathways.
The RAS-ERK pathway. In resting cells, inactive RAS-GDP is bound to the plasma membrane, while inactive RAF, MEK, and ERK are largely cytoplasmic. Growth factor-binding activates RTK auto-phosphorylation, generating docking sites for GRB2 adaptor molecules that recruit SOS, the GTPase exchange factor (RAS-GEF), to the membrane. SOS catalyzes RAS GTP exchange and GTP-bound RAS in turn recruits RAF to the membrane, where it gets activated. RAF activates MEK and MEK activates ERK via activation loop phosphorylation. ERK also feeds back to negatively regulate the pathway. The PI3K-mTOR pathway. In quiescent cells, the lipid phosphatase PTEN maintains low levels of PIP3, resulting in AKT inactivation. TSC2, in complex with TSC1 and TBC1D7, maintains RHEB in the GDP-bound state. Insulin and IGF1 bind their cognate RTKs, and subsequent receptor autophosphorylation form binding sites that then recruit IRS1/2 proteins, an adaptor protein for PI3K. Activated PI3K phosphorylates PIP2 to generate PIP3. Pleckstrin homology domains in AKT and PDPK1 recognize PIP3 and translocate to the plasma membrane. PDPK1 phosphorylates the activation loop and mTORC2 phosphorylates the hydrophobic motif of AKT, thus promoting AKT activation and phosphorylation of TSC2, which inhibits TSC2 GAP activity. RHEB-GTP localizes to the lysosome and activates mTORC1. Adapted from Mendoza *et al.* [85].

1.9 Amino acid signaling

Amino acid availability is transmitted to mTORC1 mainly via the Rags (Ras-related family of small GTPases) [92]. There are four Rag homologs in mammals (RagA/B/C/D) that form obligate heterodimers of RagA or RagB with RagC or RagD. Rags are attached to the lysosomal limiting membrane through the pentameric LAMTOR complex composed of LAMTOR1-5 [93, 94]. There are two sets of obligate heterodimers in the complex, LAMTOR2 and 3, which are positioned right above LAMTOR4 and 5. LAMTOR1 wraps around the other subunits, providing structural support and keeping the heterodimers in place [95, 96]. Amino acid sufficiency promotes the mTORC1-activating conformation of the Rag heterodimers (RagA/B^{GTP}, and RagC/D^{GDP}). The active Rag heterodimer binds RAPTOR and thereby recruits

mTORC1 from the cytosol to the lysosomal surface [97, 98]. Structural analyses have revealed that the region in RAPTOR comprising amino acids 546–650 binds $RagA^{GTP}$, while two additional regions of RAPTOR, located between the ARM and WD40 b-propeller domains, interact with $RagC^{GDP}$, spanning amino acids 795–806 and 916–937, respectively [97]. The nucleotide-binding status of the Rags is tightly regulated by conserved GAPs and GEFs. The heterotrimeric GAP activity toward Rags-1 (GATOR1) complex composed of NPRL2, NPRL3, and DEPDC5 is the GAP for RAGA/B and thus negatively regulates mTORC1 activity [99]. GATOR1 is tethered to the lysosomal surface by KICSTOR (KPTN, ITFG2, C12orf66, and SZT2-containing regulator of mTORC1 [100]. The heteropentameric complex GATOR2 (WDR24, MIOS, WDR59, SEH1L, and SEC13) can activate mTORC1 by negatively regulating GATOR1 upon direct interaction [101]. The lysosomal amino-acid transporter SLC38A9 acts as a GEF for RagA [102]. The LAMTOR complex, which was initially described as the GEF for RagA/B, was later proposed to activate mTORC1 by accelerating the release of GTP from RagC, while the identity of the GEF for RagC/D remains unclear [102]. Folliculin (FLCN) together with its binding partners folliculin-interacting protein 1 and 2 (FNIP1/2), has been identified as the GAP for RagC/D and thus positively regulates mTORC1 [103]. Upon amino acid withdrawal, the Rag heterodimer assumes an inactive configuration ($RagA/B^{GDP}$ and $RagC/D^{GTP}$) that is unable to recruit mTORC1 to the lysosomal surface so that mTORC1 remains cytosolic [101, 104]. Intriguingly, the TSC complex can form direct interactions with the Rag GTPases in an amino acid-dependent manner. The interface for such an occasion was shown to involve the preferential binding of TSC2 to $RagA^{GDP}$. Amino acid deprivation relocalizes TSC to the lysosomal surface, whereupon it facilitates the release of mTORC1 to the cytosol. Cells lacking TSC2 fail to completely dissociate mTORC1 from the lysosome resulting in incomplete mTORC1 inhibition during amino acid scarcity (Figure 1.5) [67].

1.10 Amino-acid sensors

Mammalian cells have evolved a sophisticated system to detect changes in specific amino acids and ensure that mTORC1 only engages in protein synthesis when sufficient amino acid building blocks are available. SESTRIN2 and SAR1B are the

amino acid sensors for leucine, whereas CASTOR1 and SLC38A9 bind and transmit the availability of cytosolic and lysosomal arginine, respectively [100, 105-107]. When leucine is limiting, SESTRIN2 binds and inhibits GATOR2 [100]. GATOR1 maintains the Rag heterodimer inactive, preventing mTORC1 recruitment to lysosomes and its activation. Leucine repletion disrupts the SESTRIN2-GATOR2 interaction, liberating the Ring domain of the WDR24 E3 ligase [104]. WDR24 recruits the E2 ligases UBE2J2 and UBE2D3 to ubiquitinate the catalytic subunit NPRL2 and inactivate GATOR1. Besides SESTRIN2, SAR1B was also shown to suppress mTORC1 by binding and inhibiting GATOR2 [108]. However, SAR1B binds to leucine with higher affinity than SESTRIN2 (K_d of 2 μM v K_d of 20 μM). This increased sensitivity of SAR1B for sensing leucine could be relevant in tissues where leucine constitutes a potent stimulator of protein synthesis e.g., skeletal muscle, in order to maintain basal mTORC1 activity when leucine levels are low [108]. Similar to the mechanism of leucine sensing by SESTRIN2, cytosolic arginine disrupts the binding of CASTOR1 to GATOR2 [105]. However, the molecular details leading to GATOR2 inhibition remain poorly defined. SLC38A9 monitors amino acid levels in the lysosomal lumen and defines the lysosomal branch of the nutrient sensing machinery [106, 107]. SLC38A9 spans the lysosomal membrane via 11 transmembrane helices and transports leucine and other non-polar essential amino acids out of the organelle in an arginine-gated fashion [107, 109]. Binding of arginine allosterically promotes the interaction of SLC38A9 through its cytosol-facing N-terminal domain with the LAMTOR complex and Rag GTPases stabilizing RagA/B to the active state [102]. Finally, although not a *bona fide* amino acid sensor, S-adenosylmethionine sensor upstream of mTORC1 (SAMTOR), a cytosolic protein that senses the methionine derivative S-adenosylmethionine (SAM), negatively regulates mTORC1 by binding GATOR1 and KICSTOR under methionine or SAM deprivation [110, 111]. Restoring SAM levels causes the dissociation of SAMTOR from these complexes to stimulate mTORC1 activity (Figure 1.5).

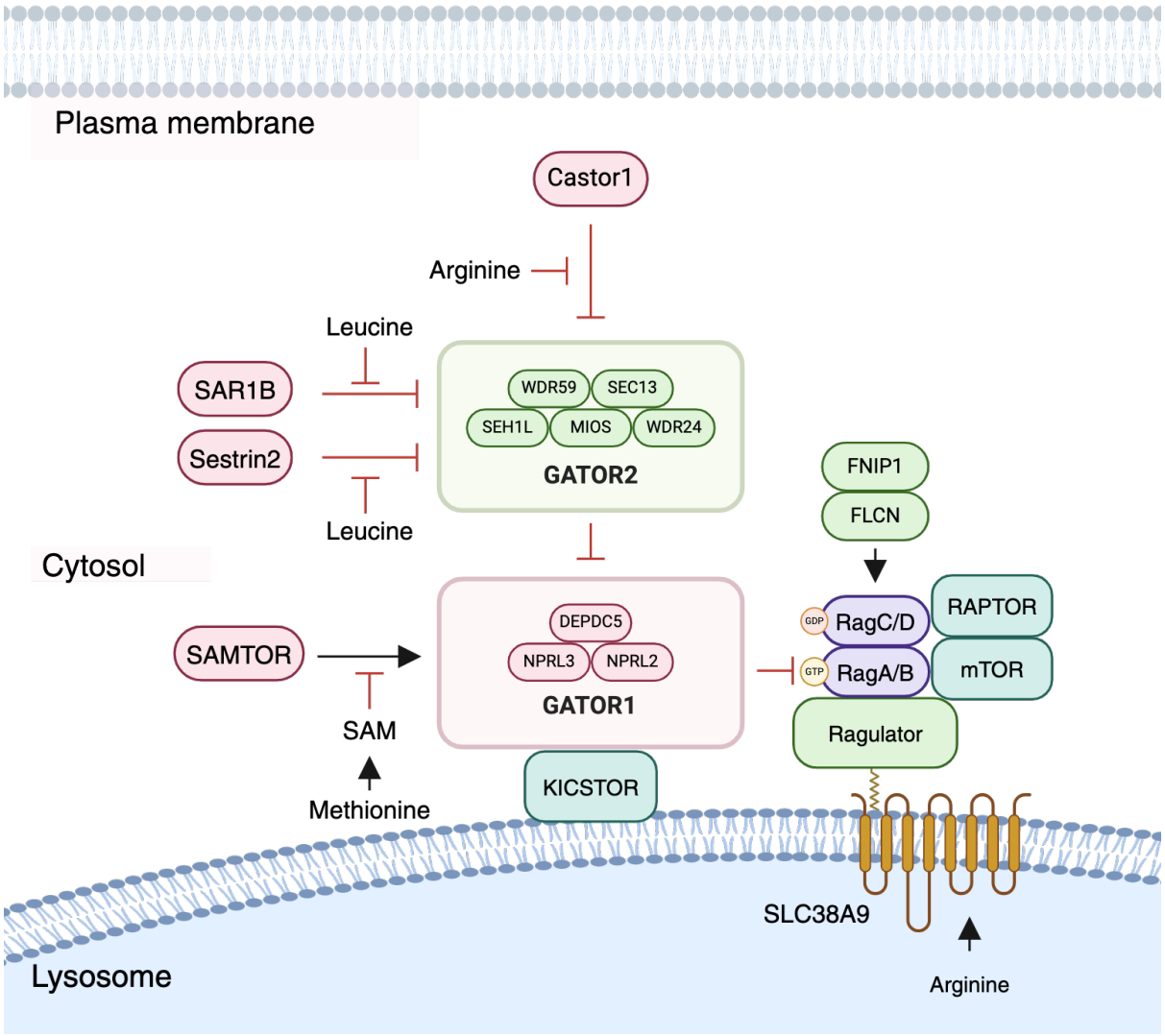

Figure 1.5. mTORC1 lysosomal amino acid sensing machinery.
In the absence of leucine or arginine, Sestrin2 and CASTOR1, respectively, bind to GATOR2, preventing it from inhibiting the RagA/B-GAP activity of GATOR1. Lysosomal arginine modulates the interaction of SLC38A9 with the Rag GTPases, favoring their transition to the mTORC1-activating state. Low levels of methionine, leucine, and arginine individually inhibit the recruitment of mTORC1 to the lysosome. When methionine is limiting, SAMTOR associates with KICSTOR and GATOR1, stimulating its GAP activity toward RagA/B. Meanwhile, GDP-bound RagA/B keeps the folliculin (FLCN)–FLCN-interacting protein 2 (FNIP2) heterodimer in an inactive state, blocking its GAP activity toward RagC/D and thus maintaining RagC/D in the GTP-bound state. [17, 112].

1.11 Energy sensing

Cell growth requires sufficiently high levels of cellular energy in the form of ATP to sustain biological processes for the synthesis of macromolecules including lipids, proteins, and nucleotides, all of which fall under the regulation of mTORC1. Therefore, it should come as no surprise that mTORC1 signaling is very sensitive to fluctuations in the relative abundance of AMP and ADP to ATP. Correspondingly, AMP-activated protein kinase (AMPK), the major energy sensor, has been shown to modulate mTOR signaling by forming several signaling branches with components of the lysosomal

sensing machinery, mTORC1 itself, or the TSC complex. Earlier studies had hinted at the role of AMPK activation in mTORC1 signaling in a Rag-dependent fashion. To this end, mutations of RagA/B that abolish GTPase activity completely abrogated inhibition of mTORC1 by glucose starvation, despite intact activation of AMPK [113]. More recently, AMPK was shown to directly phosphorylate WDR24 on S155 disrupting the integrity of the GATOR2 complex to suppress mTORC1 activity [114]. In line with the role of AMPK in suppressing mTORC1 in a Rag-dependent manner, AMPK directly phosphorylates five conserved serine residues on FNIP1, suppressing the function of the FLCN-FNIP1 GAP complex, which results in the dissociation of RagC and mTORC1 from the lysosome [115]. Furthermore, AMPK directly phosphorylates RAPTOR at two sites, S722 and S792 resulting in 14-3-3 binding to RAPTOR and inhibition of mTORC1 kinase activity. Mutation of these two sites was found to reduce the ability of the AMPK activators, AICAR or phenformin, to inhibit S6K1 and 4EBP1 phosphorylation, although the molecular mechanism for this inhibitory effect remains elusive [116, 117]. Lastly, AMPK phosphorylates TSC2 at T1271 and Ser1387. Introduction of a phospho-deficient mutant mitigates the effect of the glycolytic inhibitor 2-deoxyglucose on mTORC1 inhibition. Notably, this phosphorylation is sometimes assumed to promote the GAP activity of the TSC complex toward RHEB, although this has not been directly demonstrated (Figure 1.6) [118].

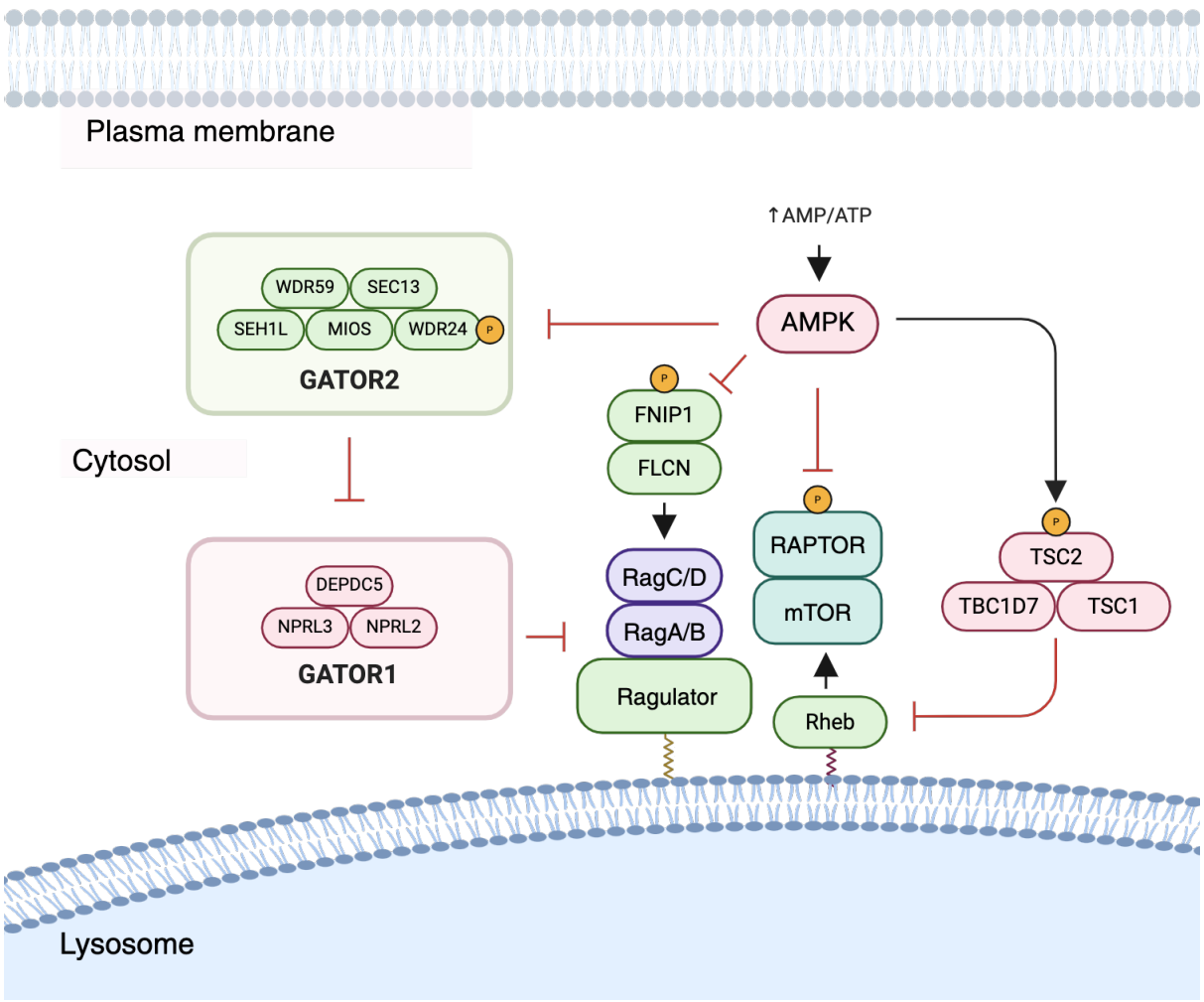

Figure 1.6. AMPK-mediated phosphorylation events inhibit mTORC1 signaling.
AMPK phosphorylates TSC2 on T1271 and S1387 to promote its GAP activity toward RHEB. AMPK also phosphorylates RAPTOR on S722 and S792 to inhibit mTORC1. Phosphorylation of WDR24 on S155 destabilizes GATOR2 through the recruitment of 14-3-3 anchor proteins. FNIP1 phosphorylation on several serine residues prevents FLCN from converting RagC/D to its "active" GDP-bound state, interfering with mTORC1 lysosomal localization [79, 115].

1.12 mTORC2 signaling and regulation

In contrast to mTORC1, growth factor signaling alone is sufficient to activate mTORC2, but the mechanism is still incompletely understood. Insulin promotes the activation of PI3K and production of PIP3, which in turn binds mSIN1 to relieve a mSIN1-mediated inhibitory effect on mTORC2 [119]. While mTORC1 regulates cell growth and metabolism, mTORC2 instead controls proliferation and survival primarily by phosphorylating several members of the AGC (PKA/PKG/PKC) family of protein kinases. The first mTORC2 substrate to be identified was PKCa, a regulator of the actin cytoskeleton [120, 121]. The most important role of mTORC2, however, is likely the phosphorylation and activation of AKT [122]. Once active, AKT promotes cell

survival, proliferation, and growth through the phosphorylation and cytoplasmic sequestration of the FOXO1/3a/4 transcription factors, thus preventing the expression of their target genes. Finally, mTORC2 also phosphorylates and activates SGK1, another AGC-kinase that regulates ion transport as well as cell survival [123].

1.13 mTOR signaling in disease

It is well-established by now that mTORC1 aberrant signaling is implicated in a variety of human diseases, including – among others – diabetes, neurological disorders, and cancer [124]. Indeed, genetic lesions that drive tumorigenesis are commonly found within the RAS, PI3K, and AMPK signaling branches. Interestingly, p110α, the catalytic subunit of PI3K (PIK3CA), is the most frequently mutated single oncogene, while PTEN, the major negative regulator in the PI3K-AKT pathway, is the second most mutated tumor suppressor gene following TP53 [36]. While the TSC tumor suppressors are infrequently mutated in sporadic cancers, a large network of the most common oncogenes and tumor suppressors underlying human malignancies converge on the regulation of the TSC complex. Thus, the TSC complex is predicted to be dysfunctional in at least half of human cancers across nearly all lineages, owing to perturbations in upstream signaling pathways, resulting in chronic activation of mTORC1. Along these lines, mTORC1 hyperactivation has been reported to occur in up to 70% of human cancers [125]. In order to prevent the deleterious effects of mTORC1 dysregulation, cells rely on the presence of negative feedback loops that serve to keep the mTOR network homeostatically balanced to prevent cell-autonomous growth [126].

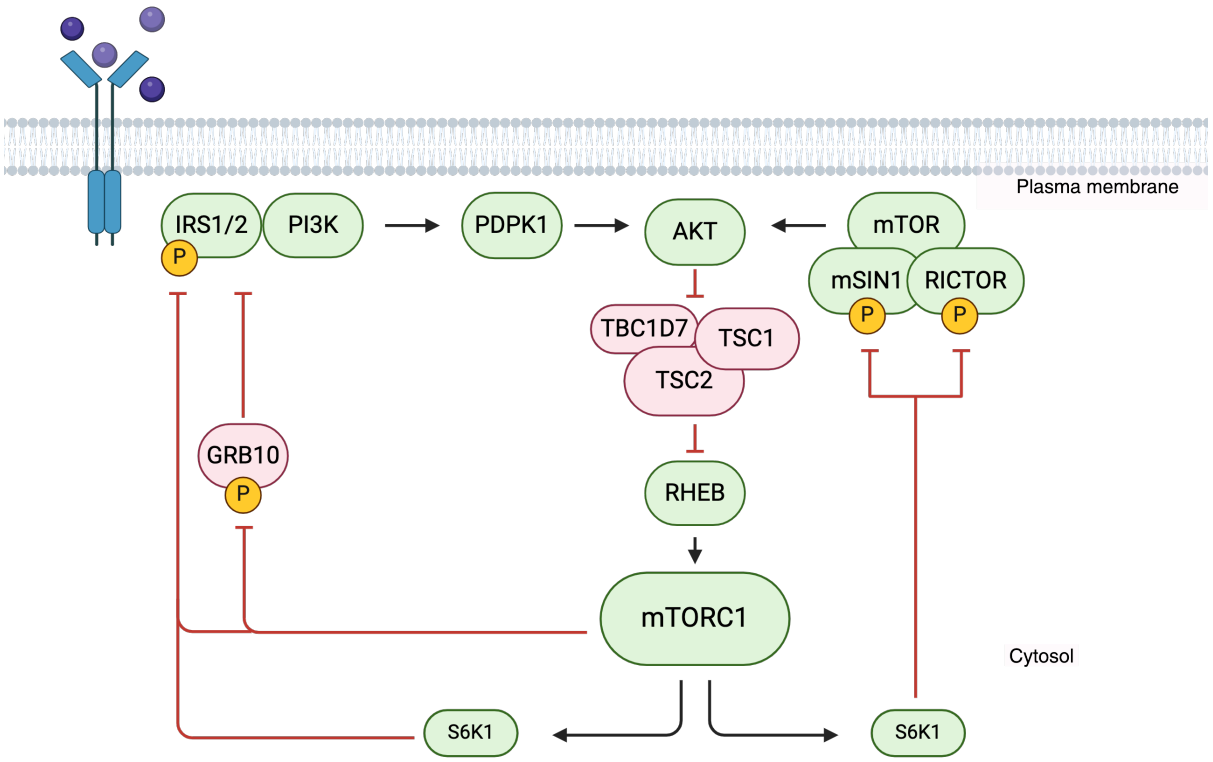

Figure 1.7. Feedback inhibition downstream of mTORC1.
mTORC1 regulates the activity of upstream signaling effectors through direct inhibition of IRS1/2, GRB10-dependent inhibition of IRS1/2, and S6K1-mediated inhibition of mTORC2 through RICTOR and mSIN1.

1.14 mTOR feedback regulation

There are four different feedback loops downstream of mTORC1, that involve the phosphorylation of IRS1/2, growth-factor-bound protein 10 (GRB10), RICTOR, and mSIN1. Activated mTORC1 and S6K1 directly phosphorylate IRS1 and IRS2 adaptor proteins on several key serine residues to promote their degradation. This reduces the ability of growth factors to signal downstream of RTKs as a result of perturbed PI3K recruitment to the plasma membrane [127-129]. Furthermore, mTORC1 activity stabilizes growth factor receptor-bound protein 10 (GRB10) upon phosphorylation, an inhibitor of PI3K signaling. GRB10 sterically hinders the association of PI3K with IRS1/2 interfering with insulin signaling [130, 131]. Sustained mTORC1 inhibition in response to physiological or pharmacological means causes compensatory over-activation of upstream lipid second messengers that serve to further activate signaling effectors thus restoring mTORC1 activity. Interestingly, mTORC1 signals to the mTORC2 subunits RICTOR and mSIN1 in a S6K1-dependent manner. RICTOR phosphorylation on T1135 promotes the recruitment of 14-3-3 anchor proteins, which

dampens the ability of mTORC2 to phosphorylate AKT on S473 in response to growth factors [132]. On the other hand, mSIN1 phosphorylation on T89 and T398 has a more drastic effect on the activity and integrity of the complex by causing mSIN1 to dissociate, thus abolishing mTORC2 signaling (Figure 1.7) [133].

2 Aims

mTORC1 integrates a wide variety of environmental cues to regulate cellular growth, including anabolic hormones, energy levels, oxygen status, and amino acids. The mechanisms by which mTORC1 largely assimilates these diverse stimuli involve signaling pathways that relay the status of these conditions through specific phosphorylation events on the TSC complex. Notably, genetic deletion of either TSC1 or TSC2 leads to constitutive activation of mTORC1, making it unresponsive to perturbations in cellular growth conditions, highlighting the crucial role of the TSC complex in orchestrating mTORC1 activity.

When nutrient reserves are limiting, feedback regulation of upstream signaling effectors involving lipid second messengers and mTORC2 leads to compensatory activation of the PI3K-AKT pathway upstream of the TSC complex to restore mTORC1 basal activity and maintain essential cellular functions. Conversely, constitutive mTORC1 activation engages the same feedback mechanisms keeping the mTOR pathway homeostatically balanced by terminating upstream signaling events.

During the course of my studies, I made the intriguing observation that in cells transiently expressing RHEB, TSC1 mobility on a polyacrylamide gel was delayed due to phosphorylation. RHEB is the immediate upstream positive regulator of mTORC1. Because mTORC1 activity would otherwise promote feedback inhibition upstream of the TSC complex, these findings raised the possibility that mTORC1 directly or indirectly drives TSC1 phosphorylation independent of the PI3K-AKT and RAS signaling axes.

Given the importance of these findings, the present thesis aims to further explore the role and context of these events by elucidating the mechanisms by which mTORC1 activity leads to TSC1 phosphorylation. Using biochemical and MS-based approaches, I characterized the molecular machinery, as well as the sites on TSC1 that are responsible for these events. Furthermore, to determine the functional implications of TSC1 phosphorylation, I generated TSC1 phospho-mutants for the identified sites and

evaluated their impact on cell physiology. Results from this work provide a better understanding of the signaling mechanisms involved in mTORC1 auto-regulation for coordinating physiological responses to the nutrient status of the cell.

3 Results

3.1 RHEB activity drives TSC1 phosphorylation

I found that in cells transiently expressing RHEB WT or an active mutant (S16H), the electrophoretic mobility of TSC1 was delayed in a polyacrylamide gel. This effect was absent in cells expressing an inactive mutant of RHEB (I39K) suggesting that the perceived upshift in TSC1 migration was the result of increased RHEB activity in response to its elevated protein levels. Phosphorylation-dependent electrophoretic mobility shift in SDS-PAGE is a common phenomenon in cell signaling studies, that can be explained by the addition of negative charges on the phospho-acceptor site as well as the nature of the neighboring residues and consequently the decrease in the amount of SDS molecules bound to the modified protein. Accordingly, treating lysates from active RHEB-expressing cells with lambda phosphatase was able to revert the delayed mobility pattern in TSC1 implicating RHEB involvement in TSC1 phosphorylation as a result of heightened activity (Figure 3.1).

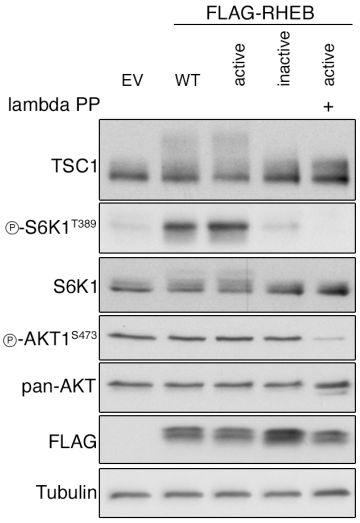

Figure 3.1. RHEB activity causes TSC1 phosphorylation.
Western blots with lysates from HEK293FT cells transiently expressing WT, active (S16H), or inactive (I39K) FLAG-tagged RHEB and probed with the appropriate antibodies. For achieving maximal electrophoretic resolution of TSC1, lysates were run on a 6% polyacrylamide gel until the 100 kDa protein marker reached the bottom of the gel. In the last lane, lysates from HEK293FT cells transiently expressing FLAG-tagged RHEB active mutant were treated with lambda phosphatase (lambda PP) for 30 min at 30°C. n = 3 independent experiments.

3.2 mTORC1 mediates the effect of RHEB on TSC1 phosphorylation

RHEB functions upstream of mTORC1 to stimulate its catalytic activity. To test whether mTORC1 mediates the effect of RHEB expression on TSC1 phosphorylation, I treated active RHEB-expressing cells for a short time course with either Rapamycin or Torin1, two pharmacological inhibitors of mTORC1. Torin1 treatment had a complete effect on rescuing TSC1 mobility after 1 hour of mTOR inhibition, indicating that mTORC1 was indeed responsible for mediating the effect on TSC1 phosphorylation, whereas cells exposed to Rapamycin only exhibited a partial response, suggesting the presence of Rapamycin-resistant sites (Figure 3.2A). Interestingly, active RHEB expression had a similar effect on TSC1 phosphorylation in U2OS cancer cells, which, could be rescued by short-term Torin1 treatment (Figure 3.2B).

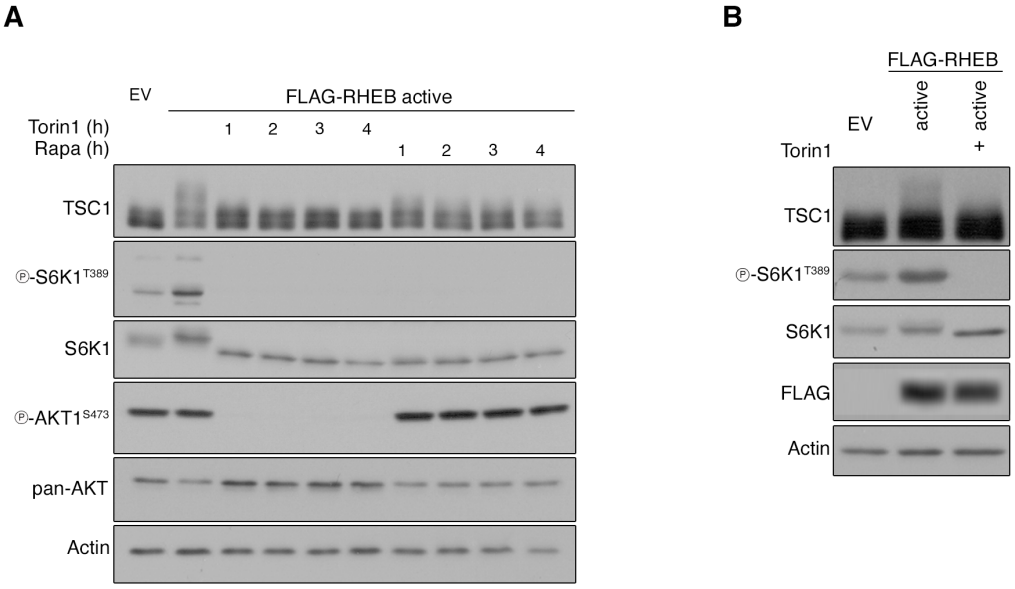

Figure 3.2. mTORC1 mediates TSC1 phosphorylation in response to RHEB activity.
(A) Western blots with lysates from HEK293FT cells transiently expressing active (S16H) FLAG-tagged RHEB, treated with Rapamycin (20 nM) or Torin1 (250 nM) for different time points and probed with the appropriate antibodies. *n* = 3 independent experiments.
(B) Western blots with lysates from U2OS cells transiently expressing active (S16H) FLAG-tagged RHEB, treated with Torin1 (250 nM) for 1 hour and probed with the appropriate antibodies. *n* = 3 independent experiments.

3.3 TSC complex integrity is required for TSC1 phosphorylation

To test whether the observed TSC1 phenotype is a result of up-regulated mTOR pathway or is exclusively the outcome of RHEB activity, I generated HEK293FT cells lacking TSC2. In such case, mTORC1 remains constitutively active even when conditions are not permissive inside the cell such as during nutrient or growth factor scarcity. Intriguingly, although transient RHEB over-expression was able to bring about a similar response in TSC2 KO cells in up-regulating mTORC1 signaling, TSC1 mobility was unaffected in the absence of TSC2. Even more surprising was the dominant negative effect that TSC2 loss had on the ability of RHEB-expressing cells to promote TSC1 phosphorylation (Figure 3.3). These results raised the possibility that TSC complex integrity might play an important role in TSC1 phosphorylation.

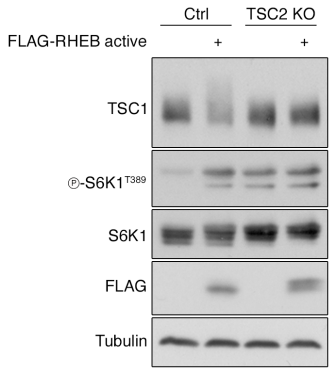

Figure 3.3. TSC2 loss abrogates TSC1 phosphorylation in cells with hyperactive mTORC1.
Western blots with lysates from HEK293FT Ctrl and TSC2 KO cells transiently expressing EV or active (S16) FLAG-tagged RHEB, grown under basal conditions, and probed with the appropriate antibodies. n = 3 independent experiments.

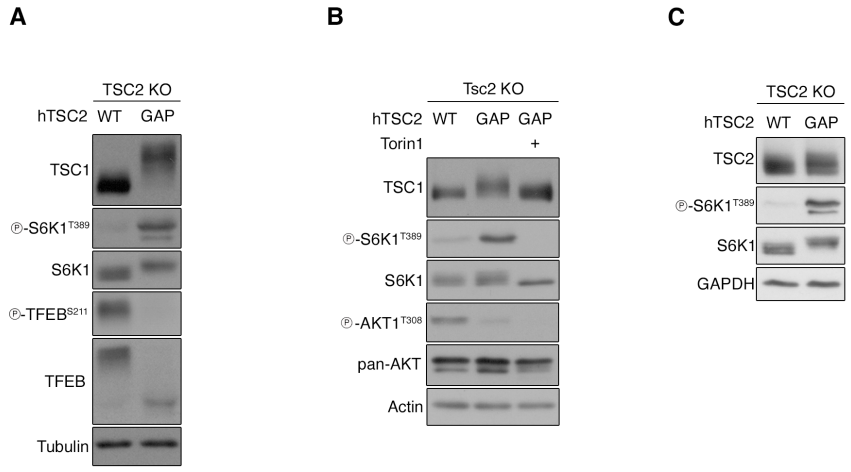

Figure 3.4. Upregulation of the mTOR pathway drives TSC1 phosphorylation.
(A) Western blots with lysates from HEK293FT TSC2 KO cells stably expressing hTSC2 WT or N1643K GAP inactive mutant, grown under basal conditions, and probed with the appropriate antibodies. *n* = 3 independent experiments.
(B) Western blots with lysates from MEF Tsc2 KO cells stably expressing hTSC2 WT or N1643K GAP inactive mutant, treated with Torin1 (250nM) for 1 hour as indicated and probed with the appropriate antibodies. *n* = 3 independent experiments.
(C) Western blots with lysates from HEK293FT TSC2 KO cells stably expressing hTSC2 WT or N1643K GAP inactive mutant probed with the appropriate antibodies. *n* = 3 independent experiments.

To test this, I analyzed the effect of a single amino acid substitution (N1643K) embedded in the TSC2 GAP domain found in human patients with Tuberous Sclerosis that renders TSC2 catalytically inactive but does not interfere with TSC complex formation. Indeed, stable reconstitution of TSC2 KO cells with TSC2 GAP inactive mutant was sufficient to elicit a complete response in the presence of hyperactive mTORC1, phenocopying the effect of transient RHEB over-expression on TSC1 phosphorylation (Figure 3.4A). Interestingly, Tsc1 phosphorylation was up-regulated in MEF cells indicating that this is a conserved event across species (Figure 3.4B). Lastly, TSC2 mobility was also shown to be delayed on a gel in an mTORC1-dependent manner but to a much lesser extent (Figure 3.4C). Due to the fact that the effect on TSC1 was substantially more pronounced, I focused on elucidating the signaling events downstream of TSC1 phosphorylation. All in all, these results indicate that up-regulation of the mTOR pathway drives TSC1 phosphorylation.

In order to establish the functional implications of TSC1 phosphorylation, I sought to characterize the sites responsible for these events. To this end, TSC1-IP coupled with

mass spectrometry (MS) led to the identification of T1047 and S1080 as two putative residues immediately downstream of the coiled-coil domain in the carboxy-terminus of TSC1. To determine whether these sites are mTORC1-dependent, I generated a phospho-antibody designed to recognize the epitope surrounding S1080 in the full-length human TSC1. I found that an increase in TSC1 phosphorylation on S1080 correlated with mTORC1 signaling in TSC2 KO cells expressing TSC2 GAP inactive mutant (Figure 3.5A). Immediately downstream of T1047 there is a proline residue (E_{1044}LSTPEK), which is in line with mTOR being a proline-directed kinase [134]. By using a phospho-threonine-proline antibody that detects phospho-threonine only when followed by proline, I was able to show that mTORC1 activity regulates the phosphorylation status of threonine-proline residues on TSC1 as an indirect validation for our predicted phosphosites (Figure 3.5B).

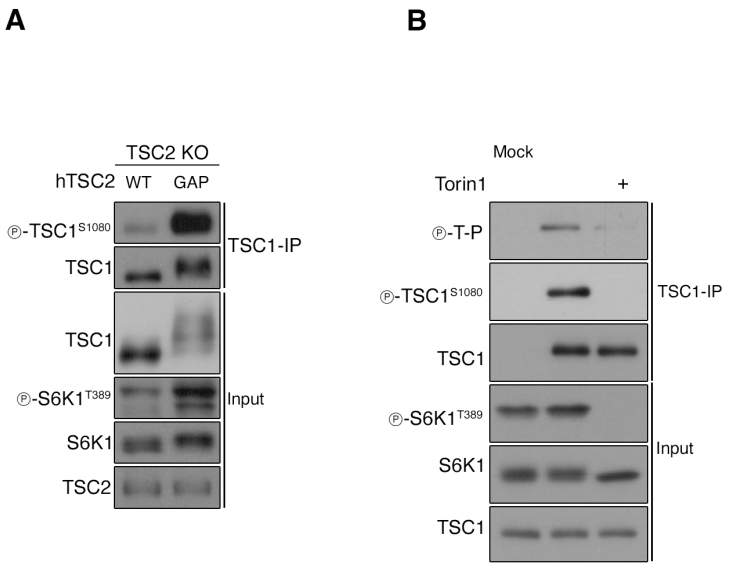

Figure 3.5. mTORC1 hyperactivity causes an increase in TSC1 phosphorylation on S1080.
(A) Western blots with lysates from HEK293FT TSC2 KO cells stably expressing WT or N1643K GAP inactive mutant, grown under basal conditions, and probed with the appropriate antibodies. For the TSC1 blot in the IP fraction, lysates were run on an 8% polyacrylamide gel until the dye front reached the bottom of the gel. For the TSC1 blot in the input, lysates were run on a 6% polyacrylamide gel until the 100 kDa protein marker reached the bottom of the gel. $n = 3$ independent experiments.
(B) Western blots with lysates from MEF cells, grown under basal conditions, treated with Torin1 (250 nM) for 1 hour as indicated and probed with the appropriate antibodies. $n = 3$ independent experiments.

3.4 TSC1 is a novel substrate of mTORC1

Next, I decided to test the hypothesis that TSC1 is a direct substrate of mTORC1. Due to its high molecular weight, a truncated version of TSC1 encoding amino acids 989 through 1163 was bacterially-purified and utilized in an *in vitro* kinase assay. I was able to successfully detect the phosphorylation of S1080 on immunopurified endogenous mTOR, which was abolished by the addition of Torin1, thus providing direct evidence for S1080 being an mTOR site (Figure 3.6). These results not only validate the MS data but also confirm that TSC1 is a novel mTORC1 substrate.

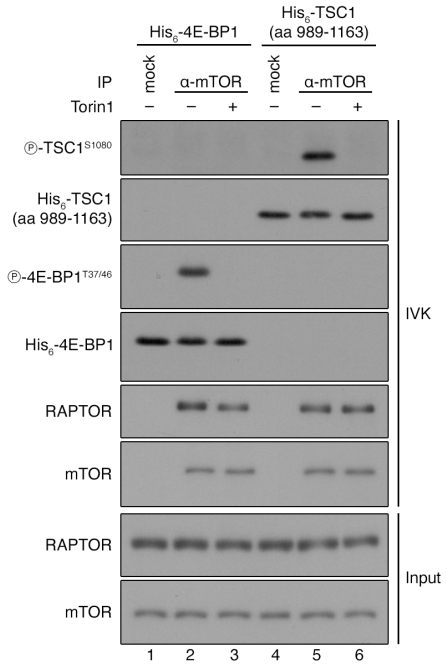

Figure 3.6. mTOR phosphorylates TSC1 in vitro.
In vitro kinase assay with endogenous mTOR immunopurified from HEK293FT cells. A truncated version of recombinant TSC1 and full-length recombinant 4E-BP1 proteins were used as substrates. Immunopurified mTOR was treated with Torin1 (5 μM) for 10 min at room temperature. $n = 2$ independent experiments.

Along the same lines and to corroborate the direct nature between the TSC complex and mTORC1, I decided to probe for an interaction between the two complexes. To address this, I carried out a co-IP experiment in which I ectopically expressed HA-tagged RAPTOR, a unique accessory component of mTORC1. TSC1 and TSC2 were enriched in the HA-IP fractions suggesting that the two complexes can interact with one another (Figure 3.7A). Previously, Manning and colleagues have demonstrated

that mTORC2 directly interacts with the TSC complex [135]. In my experiments, HA-RAPTOR was able to co-IP RICTOR – a defining subunit in mTORC2. This suggests that the two mTOR complexes can form higher order structures, raising the possibility that the enrichment of TSC1 and TSC2 in the HA-RAPTOR IP-fractions is the result of mTORC2-TSC binding. To tackle this, I performed the same HA-RAPTOR co-IP experiment as before, this time in the presence of RNAi against RICTOR. RICTOR depletion did not interfere with the binding of the TSC complex to RAPTOR demonstrating that this is a specific interaction with mTORC1 (Figure 3.7B).

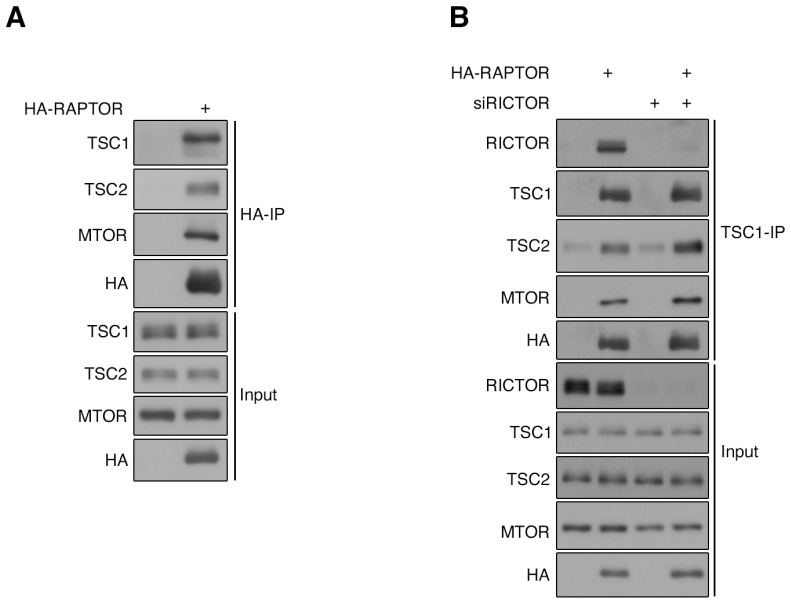

Figure 3.7. mTORC1 interacts with the TSC complex.
(A) Western blots with lysates from HEK293FT, grown under basal conditions transiently expressing HA-RAPTOR or ctrl vector. The input and IP fractions were analyzed by immunoblotting using the appropriate antibodies. *n* = 3 independent experiments.
(B) Western blots with lysates from HEK293FT transiently transfected with HA-RAPTOR or a ctrl vector in the presence of siRNAs against RICTOR or an siRNA duplex (ctrl), and probed with the appropriate antibodies. *n* = 1 independent experiment.

TSC complex integrity is necessary for TSC1 phosphorylation because the lack of TSC2 hinders mTORC1 signaling toward TSC1 (Figure 3.3). Based on that premise, I reasoned that TSC2 scaffolds the interaction between mTORC1 and the TSC complex. To tackle this, I co-expressed HA-RAPTOR in combination with a mutant version of TSC2 in which the first 424 amino acids corresponding to the TSC1 binding domain had been excised. Interestingly, I found that not only TSC1 but also mutant TSC2

could bind to mTORC1 independently of each other, suggesting that TSC complex integrity is dispensable for the interaction with mTORC1 (Figure 3.8).

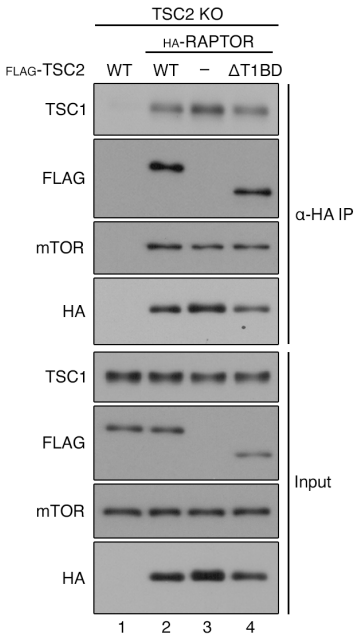

Figure 3.8. TSC complex integrity is dispensable for binding to mTORC1.
Western blots with lysates from HEK293FT TSC2 KO cells, grown under basal conditions, transiently co-transfected with ctrl vector or HA-tagged RAPTOR together with FLAG-tagged hTSC2 WT or a TSC2 mutant lacking the TSC1 binding domain corresponding to the first 424 N-terminal amino acids. The input and IP fractions were analyzed by immunoblotting using the appropriate antibodies. *n* = 3 independent experiments.

3.5 TSC1 is a novel lysosomal substrate of mTORC1

The lysosomal sensing machinery and in particular the Rag GTPases have previously been shown to mediate the recruitment of the TSC complex to the lysosomal surface upon amino acid removal. This was shown to be primarily driven by TSC2 and RagA. I speculated that lysosomal localization and binding of the TSC complex to the Rag proteins might be an important event through which mTORC1 can signal to the TSC complex similar to the lysosomal substrates, TFEB and TFE3. Intriguingly, gene silencing of RagA or RagC, but not RagB or RagD, impinged on TSC1 phosphorylation in cells with hyperactive mTORC1, while a combination of siRNAs against RagA and RagC displayed a synergistic effect. Notably, S6K1 phosphorylation was minimally affected in all of the Rag knockdown conditions (Figure 3.9).

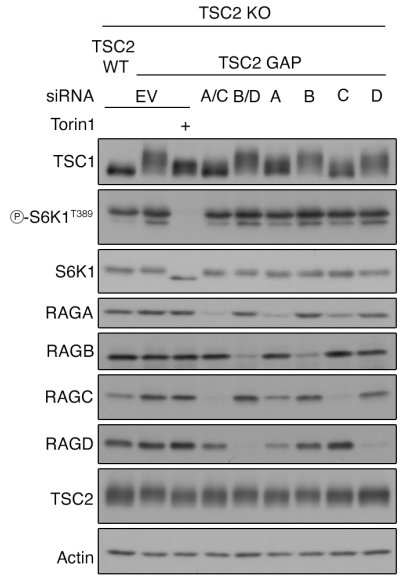

Figure 3.9. The lysosomal mTORC1 machinery is required for mTORC1 signaling to TSC1.
Western blots with lysates from HEK293FT TSC2KO cells stably expressing N1643K GAP inactive mutant transiently transfected with siRNAs against RagA, RagB, RagC, RagD or a combination of RagA/C or RagB/D, treated with Torin1 (250 nM) for 1 hour as indicated and probed with the appropriate antibodies. *n* = 3 independent experiments.

Rag proteins cycle on and off the lysosomes in a nutrient-dependent manner [136]. To address whether TSC1 phosphorylation upon RagA/C binding is a lysosomal event, I inhibited LAMTOR1 using RNAi. LAMTOR1 is a component of the LAMTOR complex that acts as a scaffold for docking Rag heterodimers to the lysosomal surface [136]. LAMTOR1 depletion led to a significant reduction in TSC1 phosphorylated species, to a similar level as Torin1 treatment (Figure 3.10A). As an independent confirmation, treatment with Bafilomycin A1, a macrolide inhibitor that blocks autophagosome – lysosome fusion and is known to inhibit mTORC1 activity specifically toward the lysosomal substrates TFEB and TFE3 [137], also diminished TSC1 phosphorylation in line with RagA/C and LAMTOR1 gene silencing (Figure 3.10B). Taken together, my results establish TSC1 as a novel lysosomal substrate of mTORC1, where TSC1 phosphorylation is down-regulated in response to any genetic manipulation or pharmacological approach that has the capacity to interfere with the lysosomal localization of the TSC complex or mTORC1.

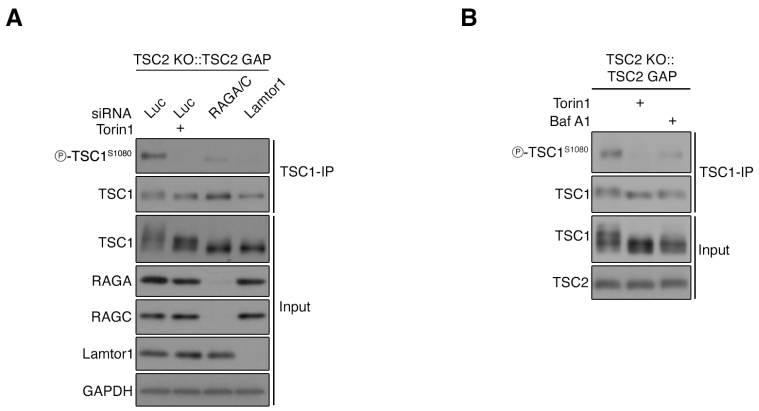

Figure 3.10. Lysosomal tethering of the TSC complex is necessary for TSC1 phosphorylation.
(A) Western blots with lysates from HEK293FT TSC2 KO cells stably expressing hTSC2 N1643K GAP inactive mutant transfected with a combination of RagA/C, LAMTOR1 or an siRNA duplex (ctrl), treated with Torin1 (250 nM) for 1 hour as indicated and probed with the indicated antibodies. *n* = 3 independent experiments.
(B) Western blots with lysates from HEK293FT hTSC2 KO cells stably expressing N1643K GAP mutant treated with Torin1 (250 nM) for 1 hour or Bafilomycin1 (100 nM) for 8 hours as indicated and probed with the appropriate antibodies. *n* = 3 independent experiments.

3.6 Physiological stresses impinge on TSC1 phosphorylation

A remarkable feature of the mTOR pathway is the wide range of intracellular and extracellular cues it integrates. To investigate whether physiological stresses that are known to inhibit mTORC1 activity can also impinge on TSC1 phosphorylation, I challenged cells by starving them for amino acids, glucose, or growth factors. In all cases, starvation resulted in a drastic decrease in TSC1 phosphorylation followed by recovery upon add-back (Figure 3.11). With these results, I was able to demonstrate that TSC1 phosphorylation, similar to other well-established markers of mTORC1 activity, responds to all environmental stresses that inhibit mTORC1.

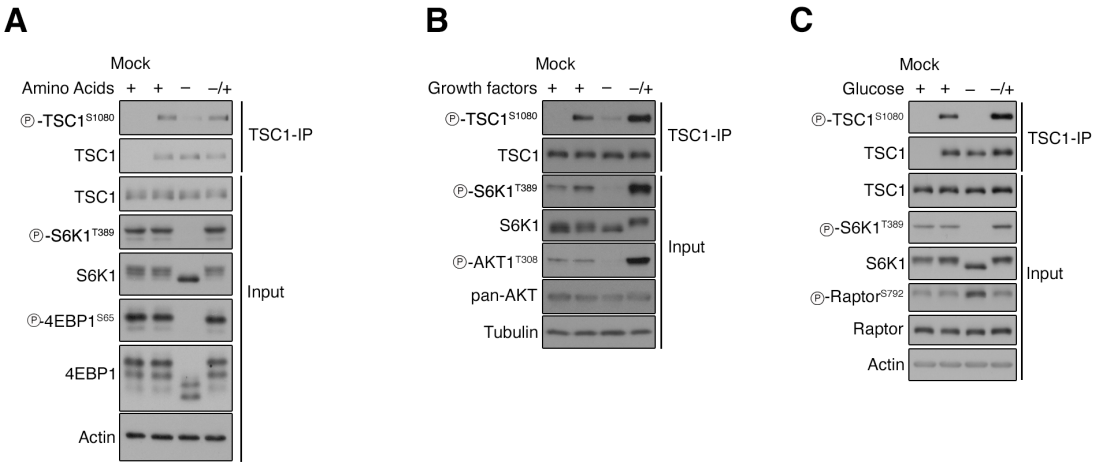

Figure 3.11. mTORC1 inhibition in response to physiological stresses diminishes TSC1 phosphorylation.
(A) Western blots with lysates from HEK293FT cells treated with media containing or lacking amino acids (AA), in basal (+), starvation (–), or add-back (–/+) conditions. *n* = 3 independent experiments. For AA starvation, culture media was replaced by starvation media 1 hour before lysis. For AA add-back, cells were first starved as described above and then starvation media was replaced by complete media for 30 minutes before lysis.
(B) Western blots with lysates from MEF cells treated with media containing or lacking FBS, in basal (+), starvation (–) or add-back (–/+) conditions. *n* = 3 independent experiments. For growth factor (GF) starvation, culture media was replaced by media lacking FBS 16 hours before lysis. For GF add-back, cells were first starved as described above and then FBS was added drop-wise at 10% final concentration, 10 minutes before lysis.
(C) Western blots with lysates from HEK293FT cells treated with media containing or lacking glucose, in basal (+), starvation (–) or add-back (–/+) conditions. *n* = 3 independent experiments. For glucose starvation, culture media was replaced by media lacking glucose 16 hours before lysis. For glucose add-back, cells were first starved as described above and then starvation media was replaced by complete media 2 hours before lysis.

Furthermore, dephosphorylation kinetics in response to mTOR inhibition upon Torin1 treatment revealed an acute drop in TSC1 phosphorylation within 10 minutes upon exposure to the drug (Figure 3.12A). In contrast, Rapamycin exerted a rather gradual response where a stronger reduction in phospho-TSC1 could be observed 3 hours after cells were subjected to the inhibitor (Figure 3.12B), which very interestingly correlated with the partial effect of Rapamycin on TSC1 delayed electrophoretic mobility depicted in Figure 3.2.

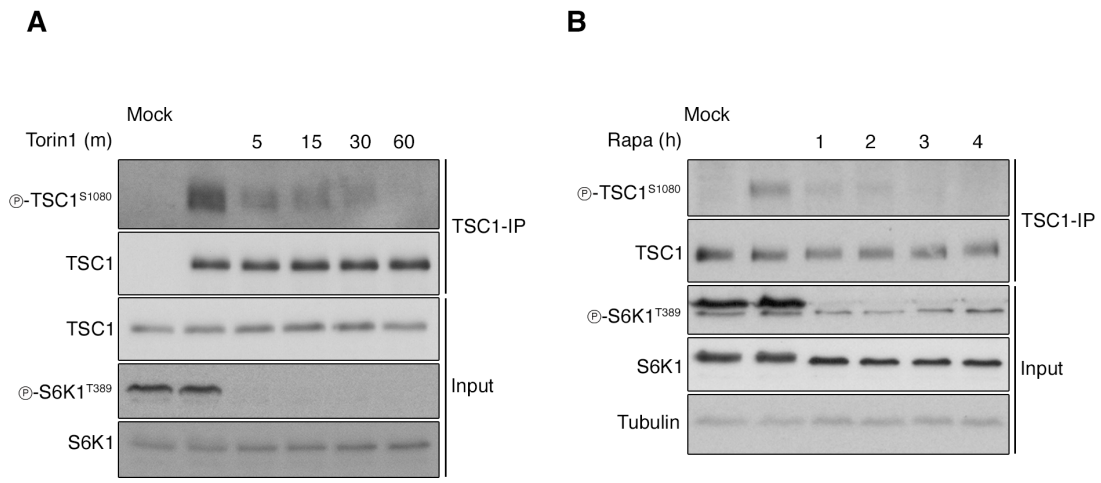

Figure 3.12. TSC1 dephosphorylation kinetics in response to pharmacological mTORC1 inhibition.
(A) Western blots with lysates from HEK293FT cells treated with Torin1 (250 nM) for the indicated time points and probed with the appropriate antibodies. *n* = 3 independent experiments. (B) Western blot with lysates from HEK293FT cells treated with Rapamycin (20 nM) for the indicated time points and probed with the appropriate antibodies. *n* = 3 independent experiments.

3.7 mTORC1 promotes TSC1 stability and binding to 14-3-3 anchor proteins

To elucidate the physiological impact of TSC1 phosphorylation, predicated on my knowledge of the phospho-acceptor residues, I generated TSC1 KO cells in which I transiently expressed WT TSC1 or a non-phosphorylatable mutant harboring alanine substitutions for the respective mTORC1 sites (TSC1-2A). TSC1 protein levels were markedly lower in cells expressing the phospho-deficient mutant, suggesting that TSC1 phosphorylation leads to changes in transcript regulation and/or protein turnover. Although differences in the mRNA abundance of WT and 2A-expressing cells could not explain the observed phenotype (data not shown), treatment with the proteasome inhibitor MG132 was able to restore TSC1 protein levels to WT, thus suggesting a role for TSC1 phosphorylation in stabilizing the protein (Figure 3.13A).

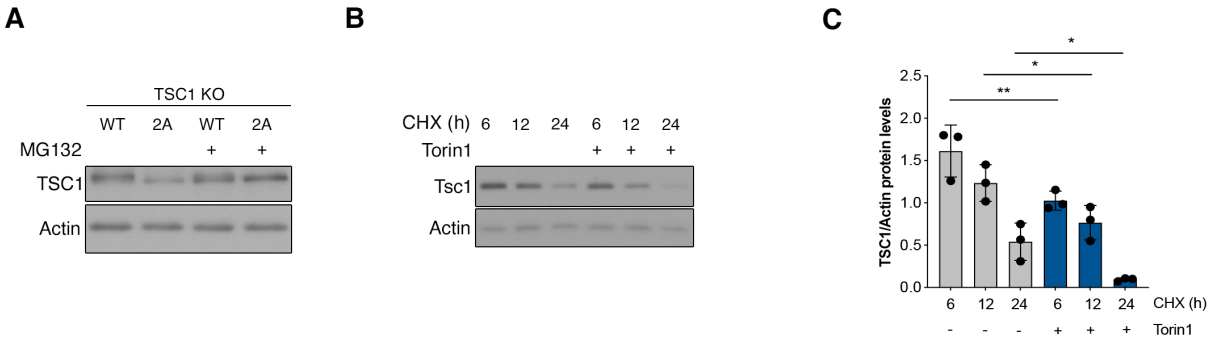

Figure 3.13. TSC1 phosphorylation promotes its stability.
(A) Western blots from HEK293FT TSC1 KO transiently expressing TSC1 WT or 2A mutant, treated with DMSO or MG132 (10 μM) for 8 hours. $n = 3$ independent experiments.
(B) Western blots from MEF cells treated with cycloheximide (CHX, 100 μM) alone or in combination with Torin1 (250 nM) for the indicated time points. $n = 3$ independent experiments.
(C) Quantified chemiluminescent signal intensity of TSC1 normalized to Actin. Data in this graph represent mean ± SD. $*p < 0.05$, $**p < 0.01$, $****p < 0.0001$.

To test whether endogenous TSC1 protein stability is negatively regulated in response to mTOR inhibition, I treated MEFs with Torin1 in the presence of cycloheximide, an inhibitor of *de novo* protein synthesis in eukaryotes. In keeping with the genetic results obtained before, cells subjected to a combinatorial treatment displayed decreased stability of endogenous TSC1 protein than cells exposed to cycloheximide alone (Figure 3.13B).

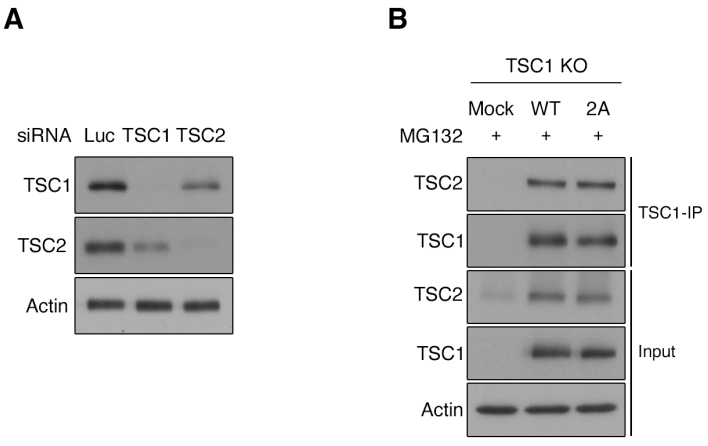

Figure 3.14. Decreased TSC1 protein stability is not due to weaker binding to TSC2.
(A) Western blots from HEK293FT cells transiently transfected with siRNAs against TSC1, TSC2, or a siRNA duplex (ctrl) and probed with appropriate antibodies. $n = 2$ independent experiments.
(B) Western blots from HEK293FT TSC1 KO cells transiently expressing ctrl vector, TSC1-WT, TSC1-2A mutant, treated with MG132 (10 μM) for 8 hours and probed with appropriate antibodies. $n = 1$ independent experiment.

In line with previous observations demonstrating that TSC complex integrity contributes to the mutual stabilization of TSC1 and TSC2 [55], gene silencing against TSC2 had a negative impact on TSC1 protein levels and *vice versa* (Figure 3.14A). To examine whether a decrease in TSC1 protein levels in the 2A mutant is the outcome of a weaker interaction with TSC2, I performed a TSC1 co-IP experiment in TSC1 KO cells transiently expressing TSC1-WT or -2A treated with MG132. The amount of TSC2 that was found to bind TSC1 was indistinguishable between WT- and 2A-expressing cells, suggesting that TSC1 phosphorylation does not affect the integrity of the TSC complex (Figure 3.14B).

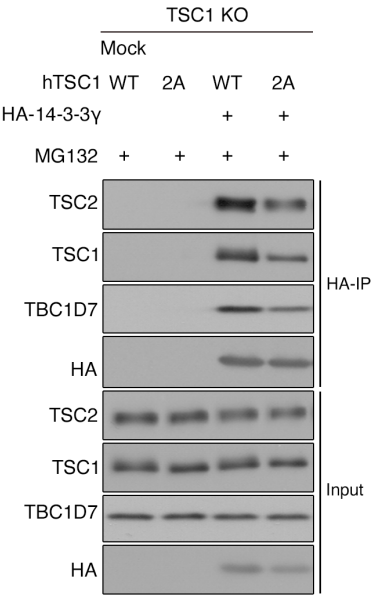

Figure 3.15. TSC1 phosphorylation promotes the binding of 14-3-3 anchor proteins to the TSC complex. Western blots from HEK293FT cells transiently expressing HA-tagged 14-3-3γ or ctrl vector, treated with MG132 (10 μM) for 8 hours and probed with the appropriate antibodies. *n* = 2 independent experiments.

The mTOR pathway can sense growth factor availability downstream of AKT through the deposition of phosphorylation marks on the TSC complex. When growth factors are sufficient, phosphorylated residues on TSC2 serve as docking sites for 14-3-3 anchor proteins, preventing the TSC complex from translocating to the lysosome and inhibiting mTORC1 [68, 82]. To test whether TSC1 phosphorylation can also dictate the binding affinity of 14-3-3s to the TSC complex, I first treated TSC1 KO cells with MG132 and then subjected lysates from WT- and 2A-expressing cells co-transfected with HA-tagged 14-3-3gamma to HA-IP. 2A-expressing cells exhibited weaker binding

of 14-3-3s to TSC1 compared with WT-expressing cells, suggesting that mTORC1 activity promotes 14-3-3 association with the TSC complex (Figure 3.15).

3.8 TSC1 phosphorylation regulates the lysosomal branch of mTORC1 signaling

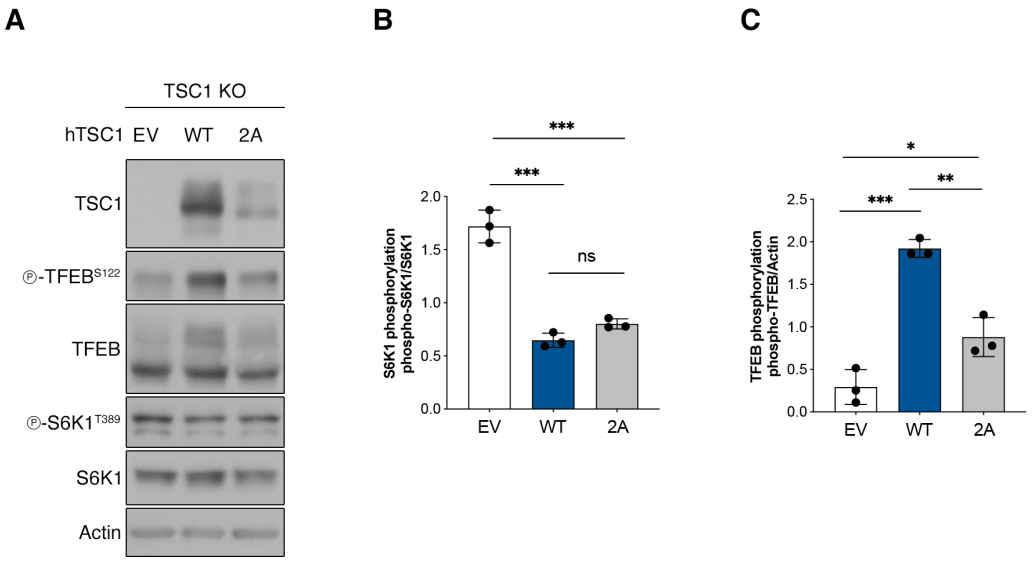

Figure 3.16. Recovery in TFEB phosphorylation is blunted in the TSC1-2A deficient mutant.
(A) Western blots with lysates from HEK293FT TSC1 KO cells transiently expressing TSC1-WT or TSC1-2A mutant, probed with the appropriate antibodies. n = 3 independent experiments.
(B) Quantified chemiluminescent signal intensity of phospho-S6K1^{T389} normalized to total-S6K1 levels. Data in this graph represent mean ± SD. $*p < 0.05$, $**p < 0.01$, $****p < 0.0001$, ns: non-significant.
(C) Quantified chemiluminescent signal intensity of phospho-TFEB^{S122} normalized to Actin. Data in this graph represent mean ± SD. $*p < 0.05$, $**p < 0.01$, $****p < 0.0001$, ns: non-significant.

TSC-deficient cells display elevated mTORC1 signaling toward non-lysosomal substrates, such as S6K1, whereas lysosomal substrates show a decrease in their phosphorylation on mTORC1-dependent sites [138]. Intriguingly, despite the apparent reduction in TSC1 protein abundance, 2A-expressing cells had seemingly similar levels of S6K1 phosphorylation relative to WT-expressing cells. On the contrary, recovery in TFEB phosphorylation was blunted upon expression of the 2A mutant, suggesting that TSC1 phosphorylation downstream of mTORC1 regulates specifically the lysosomal branch of mTORC1 signaling (Figure 3.16).

4 Discussion

The findings in this work shed light on a novel feedback mechanism of mTORC1. For more than two decades the mTOR signaling pathway has been known to operate in a linear fashion in which the TSC complex regulates the nucleotide-binding status of RHEB to control the catalytic activity of mTORC1. Based on the evidence presented here, I was able to demonstrate that mTORC1 also functions immediately upstream of the TSC complex to phosphorylate TSC1.

TSC1 phosphorylation promotes its stability and binding to 14-3-3 anchor proteins. When mTORC1 activity is suppressed, TSC1 protein levels are negatively regulated, and TSC1 is targeted for degradation via the proteasome while the binding affinity to 14-3-3s decreases. Given that the TSC complex is the major suppressor in the mTOR pathway, the directionality of these observations is in line with previous reports on feedback regulation of mTORC1, where upstream signaling effectors feed into the mTOR pathway in order to restore basal activity and maintain essential cellular functions upon prolonged absence of certain nutrients. Conversely, sustained mTORC1 hyperactivity is kept under tight control when the same upstream feedback mechanisms are terminated to finetune mTORC1 maximal signaling output that is known to be deleterious for cell physiology.

TSC1 stability was severely compromised in TSC1 KO cells ectopically expressing the non-phosphorylatable alanine mutant T1047A/S1080A for the respective mTORC1 sites. In keeping with the role of feedback regulation in finetuning mTORC1 activity, the Thompson laboratory first assigned a disruptive role to AKT in TSC complex stability, wherein upon persistent activation of an ectopic AKT mutant, both TSC1 and TSC2 protein levels were profoundly downregulated [139]. Although this might appear contradictory at first glance because active AKT would eventually spike mTORC1 signaling – that would otherwise promote TSC1 stability – essentially, this creates a constant equilibrium between the PI3K-AKT and mTOR signaling nodes in which TSC lies right at the center. In its simplest form, one would imagine the ancient game of tug-of-war whereupon sustained AKT activation causes the TSC complex to fall apart,

while active mTORC1 counteracts this effect by promoting TSC1 stability, prospering homeostasis within the mTOR pathway.

The reduction in TSC1 protein levels in the phospho-deficient mutant was accompanied by lower levels of TFEB phosphorylation. Although this is counterintuitive, dysregulation of the TSC-RHEB axis has been observed to have opposing effects on lysosomal and cytosolic substrates. It is known that in the absence of a functional TSC complex, or upon RHEB activation, TFEB phosphorylation diminishes in the presence of hyperactive mTORC1, whereas phosphorylation on S6K1 and 4E-BP1 is augmented [54, 140, 141]. Even more paradoxical is the lack of an effect on TFEB phosphorylation following growth factor depletion despite the evidence of genetic perturbations in the TSC-RHEB axis. The mechanistic details of these phenomena remain elusive.

My findings show preferential regulation of the lysosomal pool of mTORC1 targets in response to changes in the phosphorylation status of TSC1, with minimal effect on the non-lysosomal substrate S6K1. Recent work from our laboratory shed light on this discrepancy in which distinct mTORC1 entities inside the cell carry out compartmentalized signaling events under basal conditions [137]. The question that arises is what is the role of TSC1 and the TSC complex as a whole in this process. TSC complex localization is the main determinant for regulating mTORC1 activity in the presence of environmental stressors [142]. Therefore, would it not be reasonable to hypothesize that the TSC complex can operate at distinct sub-cellular locations and regulate mTORC1 locally? If so, how can a decrease in protein abundance generate such a gradient where the lysosomal pool of mTORC1 substrates responds to the presence of TSC1 phosphorylation while the non-lysosomal pool remains largely unaffected?

Besides an apparent decrease in TSC1 protein levels, 2A-expressing cells displayed weaker binding of 14-3-3 anchor proteins to TSC1. Although a clear understanding of the molecular events pertaining to TSC localization dynamics is missing, 14-3-3 anchor proteins have been previously reported to mediate in this process. The

conventional model of mTORC1 regulation downstream of growth factor signaling describes the binding of the TSC complex to 14-3-3s, leading to its sequestration in the cytosol [68, 82]. When growth factors are scarce, 14-3-3s dissociate from the TSC complex, causing it to relocalize to the lysosome. Intriguingly, Demetriades *et al*. demonstrated enhanced lysosomal enrichment of the TSC complex in response to amino acid starvation [67]. A major distinction between amino acid starvation and growth factor withdrawal concerning TSC localization is that in the case of amino acids, the TSC complex preferentially binds to GDP-loaded RagA, whereas during growth factor depletion, the TSC complex binds to RHEB. Although the authors did not demonstrate how the TSC complex is recruited to the lysosome when exogenously supplied amino acids are missing, it is tempting to speculate that the lack of mTORC1-dependent phosphorylation of TSC1 and the consequent reduction in its binding to 14-3-3s is part of the answer. To this end, I propose that apart from regulating TSC1 stability, TSC1 phosphorylation dictates its binding affinity to 14-3-3 anchor proteins in a similar manner AKT dictates the fate of the TSC complex upstream of the mTOR pathway. Upon mTORC1 inhibition, 14-3-3s dissociate from the TSC complex, which favors TSC-RagA interaction. The TSC complex antagonizes mTORC1 for binding to RagA, displacing mTORC1 from the lysosome [67]. The antiparallel between enhanced TSC complex occupancy at the lysosome coupled with mTORC1 release could explain why 2A-expressing cells display an inability to properly regulate TFEB signaling.

More recently, lysosomal tethers other than the Rag GTPases have been described to mediate TSC complex docking on the lysosome, including the G3BPs, as well as the N-terminal HEAT domain in TSC1 that recognizes and binds to phosphorylated lipid species [59, 143]. However, an intact lysosomal sensing machinery was shown to play a dominant role in mTORC1 catalysis toward TSC1. RNAi against RagA/C and LAMTOR1 reduced the ability of mTORC1 to phosphorylate TSC1, while S6K1 phosphorylation was hardly affected. Inhibiting the lysosomal V-ATPase upon exposure to Bafilomycin A1 phenocopied the effect of RagA/C and LAMTOR1 gene silencing on TSC1 phosphorylation. In line with earlier observations by Fernandes *et al*., my findings show that TSC1 is a novel lysosomal substrate of mTORC1 [137].

To put these observations into perspective, mTORC1 localization on the lysosome in the absence of environmental stressors drives local TSC1 phosphorylation and lysosomal exclusion, whereupon mTORC1 can signal unhindered to the lysosomal substrates. When conditions are restrictive, 14-3-3s can no longer prevent hypo-phosphorylated TSC1 from translocating to the lysosome due to weaker binding. The preferential binding of the TSC complex to RagA in conjunction with the altered RagA nucleotide binding state forces mTORC1 away from the lysosome, terminating the lysosomal branch of mTORC1 signaling.

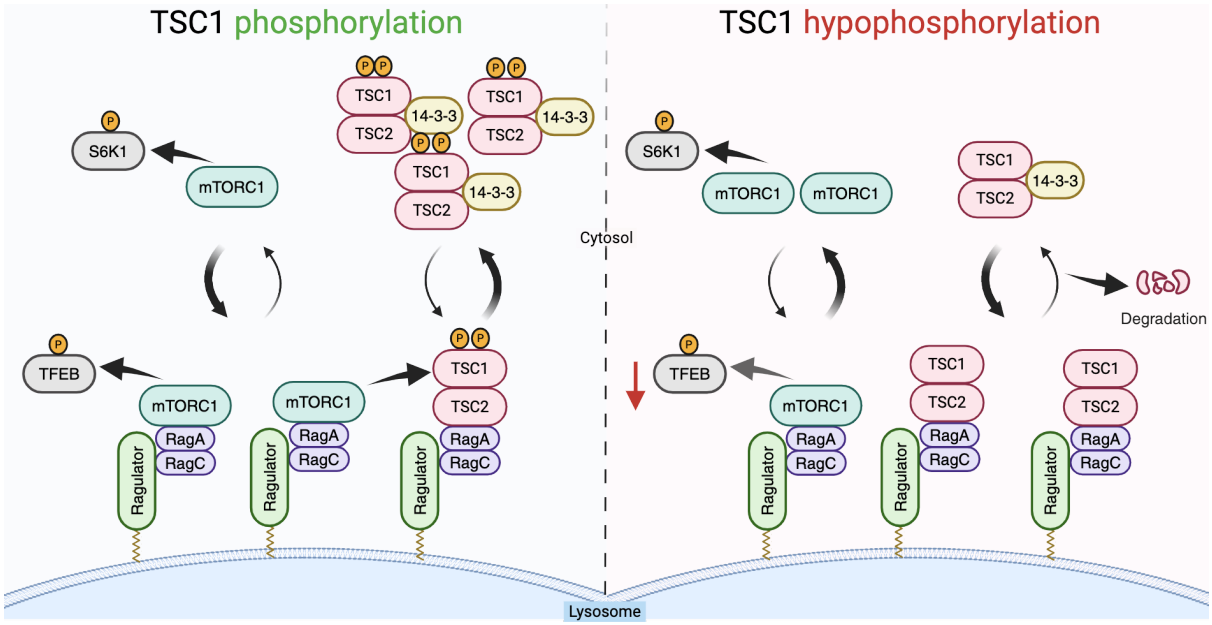

Figure 4.1. TSC1 phosphorylation on mTORC1-dependent sites promotes its stability and binding to 14-3-3 anchor proteins.
Binding to 14-3-3 proteins interferes with lysosomal localization of the TSC complex, wherein mTORC1 can signal to the lysosomal substrates. Hypophosphorylated TSC1 competes with mTORC1 for binding to RagA. As a result, mTORC1 abundance on the lysosome decreases, which suppresses TFEB phosphorylation. Sustained TSC1 hypophosphorylation leads to its proteasome-mediated degradation, which contributes further to the negative effect on TFEB phosphorylation.

A decrease in TSC1 protein abundance and its weaker binding to 14-3-3 proteins essentially elicit the same response on TFEB phosphorylation. What could be the reason for the existence of a dual mechanism that brings about the same outcome? A potential explanation other than synergy is an acute versus prolonged response. The binding of 14-3-3s to phosphorylated residues on TSC2 downstream of AKT takes place within minutes after serum re-addition, preceded by overnight starvation [68, 82].

In the case of TSC1, one could imagine that amino acid starvation followed by add-back can exert the same binding kinetics, causing a rapid shuttling of the TSC complex on and off the lysosomal surface. A second wave imposed by persistent mTORC1 inhibition causes TSC1 protein levels to drop. In such a case, TSC localization is sustained while TSC complex activity diminishes over time, ensuring that milder fluctuations in nutrient availability play a minor role in mTORC1 signaling unless basal activity is restored in replete conditions.

The relative stoichiometry of the non-lysosomal TSC complex can be a plausible explanation as to why there is no difference in the phosphorylation of canonical mTORC1 substrates. Mutagenesis of the phospho-acceptor residues to alanine had a dramatic impact on TSC1 stability. However, the relative abundance of the remaining TSC1-2A copies that were localized in non-lysosomal compartments could still be sufficient for rescuing mTORC1 signaling, even though at much lower levels than WT-expressing cells. Another possible interpretation is for technical reasons. Our results are based on transient over-expression experiments, in which case, the levels of ectopic TSC1-2A protein can be several orders of magnitude higher than that of the endogenous TSC1 levels.

It is therefore important to consider whether this apparent discrepancy between lysosomal and non-lysosomal substrates has a physiological basis in the context of my TSC1 mutant. I was able to demonstrate that in the absence of principal physiological cues that are known to regulate mTORC1 activity, namely glucose, amino acids, and growth factors, TSC1 phosphorylation is down-regulated. Using 2A-expressing cells as a tool for addressing specifically the role of TSC1 phosphorylation in mTORC1 signaling, I was able to establish that TFEB phosphorylation is negatively affected when TSC1 is hypophosphorylated. Since TSC1-2A can only exist in a setting where mTORC1 activity is low, it is logical to assume that under these conditions, the cell enters a starvation mode, shunting resources towards catabolism as it would be deleterious to invest in the phosphorylation of substrates involved in energy-consuming biosynthetic processes, such as S6K1 or 4E-BP1. Concomitantly, besides the rationale for lysosomal substrate regulation, the lack of an increase in the

phosphorylation of the non-lysosomal substrates by mTORC1 prevents the deposition of repressive phosphorylation marks on autophagy-related proteins (ULK1, ATG13, and ATG14), thus allowing for the autophagic process to carry on unperturbed.

What is the pathophysiological relevance of the TSC complex-TFEB axis? TSC patients with inactivating germline mutations in either the TSC1 or TSC2 genes experience the formation of benign lesions in multiple organ systems, including the brain, skin, heart, lungs (manifesting as lymphangioleiomyomatosis), and kidneys [144]. Renal involvement, which may present as angiomyolipomas, cysts, and, in some cases, renal cell carcinoma, constitutes the primary cause of morbidity and mortality in individuals with TSC [54, 145]. As mentioned before, in TSC1- and TSC2-deficient cells, TFEB is hypo-phosphorylated, leading to TFEB nuclear localization and transcriptional activation. Coincidentally, there is extensive evidence in the literature showing that aberrant TFEB signaling is implicated in a wide spectrum of renal pathologies underlined by chromosomal translocations in the TFEB locus, or in the case of Birt-Hogg-Dubé (BHD) syndrome, loss-of-function mutations of FLCN leading to skin tumors, lung cysts, and kidney cancer. More recently, the Henske laboratory demonstrated that whole-body or kidney-specific genetic ablation of TFEB was able to rescue renal pathology and lethality in a whole-body inducible mouse model of TSC (Tsc2 -/-) [54]. Although in the clinical setting, the disease relevance of the TSC1-TFEB axis can be overridden by the presence of homozygous TSC1 or TSC2 loss-of-function mutations, initially manifesting as heterozygous germline mutations followed by somatic inactivation of TSC1/2, second hits are not always appearing [145]. Indeed, loss-of-heterozygosity (LOH) was found to be present in only 56% of renal angiomyolipomas [57]. More than 85% of patients living with TSC harbor mutations in the TSC2 gene [145]. This raises the possibility that an increase in mTORC1 signaling associated with the loss of a functional TSC2 allele can promote TSC complex integrity by stabilizing TSC1 and alleviating disease severity.

These findings support the concept that TFEB regulation is the critical mechanistic link and potentially the primary driver of tumorigenesis in TSC, suggesting that TFEB is a critical disease-relevant target of the TSC1 and TSC2 proteins.

5 Future perspectives

5.1 Open questions based on the presented findings

Although I was able to demonstrate that a decrease in TSC1 protein levels was due to stability, it remains an open question whether or not proteasome-mediated degradation of TSC1 is a ubiquitin-dependent event and what are the effectors implicated in phospho-TSC1 recognition and targeting for degradation. I showed that the lysosomal sensing machinery is involved in TSC1 phosphorylation and that 14-3-3 proteins have a low affinity for binding to the phospho-deficient mutant. However, biochemical evidence pertaining to the role of TSC1 phosphorylation in TSC complex localization is missing and should be addressed in future studies. Moreover, TFEB phosphorylation is consistent with its spatial distribution inside the cell. Future experiments should aim at capturing the subcellular localization of TFEB and its activity toward lysosomal transcriptional targets.

TSC1 and TSC2 proteins have been shown to function in concert and genetic loss of either of the two components renders the TSC complex inactive. mTORC1 activity leads to a subtle upshift in TSC2 on a gel, which can be rescued upon mTORC1 inhibition (presented in Figure 3.4). I have preliminary evidence of identified phosphorylation sites on TSC2 that respond to mTORC1 activity based on TSC2-IP/MS experiments. In addition, during my PhD studies, I generated HEK293FT cells lacking both TSC1 and TSC2 proteins. It is intriguing to hypothesize that a synergistic effect is in place where mTORC1 directly phosphorylates TSC1 and directly or indirectly contributes to TSC2 phosphorylation orchestrating a robust feedback response to the presence of environmental stressors or upon sustained mTORC1 activation.

Exploratory concepts

5.2 mTORC1 and CDK1 signaling converge on TSC1

Previously, CDK1 activity was shown to correlate with a delayed mobility of TSC1 on a gel. CDK1 was proposed to phosphorylate TSC1 on three sites, one of which was reported to be T1047 [146]. However, in my experimental conditions, CDK1 does not

play a role in TSC1 phosphorylation in cells with active mTORC1, as Torin1 treatment in cells expressing ectopic RHEB was able to completely reverse the effect of mTORC1 hyper-activity on TSC1 mobility upshift. Furthermore, CDK1 inhibition in TSC2 KO cells stably expressing TSC2 GAP inactive mutant had no apparent effect on TSC1 phosphorylation (data not shown). Nevertheless, an overlap between CDK1 and mTORC1 in the phosphorylation of several other substrates involved in catabolic processes has been established previously [147]. Indeed, in prometaphase-arrested cells exposed to nocodazole, substrates involved in autophagy initiation and nucleation, as well as, lysosome biogenesis including ULK1, ATG13, ATG14, TFEB, and TFE3 are phosphorylated by CDK1 on mTORC1-dependent sites to ensure that autophagy is repressed during cell division [147]. This is believed to protect genome integrity during nuclear envelope breakdown and exposure to the autophagic machinery. During mitosis, mTORC1 activity is down-regulated [148]. It is, therefore, tantalizing to envision that the promiscuity in TSC1 phosphosites between CDK1 and mTORC1 serves to prevent mTORC1 from being activated during progression through mitosis due to a decrease in TSC1 protein abundance. This realization could help explain further the specificity of the TSC-TFEB axis and the lack of an effect on canonical mTORC1 targets in order to maintain low levels of lysosomal biogenesis while keeping anabolic processes at bay. In addition, mTORC1 hyper-activity in cells lacking TSC2 has been linked to accelerated G2/M checkpoint recovery, essentially raising the risk for cells entering mitosis prematurely in the presence of DNA damage [149]. Questions that would be relevant to address in future studies based on the aforementioned evidence and hypotheses include i) what are the consequences of aberrant TSC1 phosphorylation on genome integrity in cells undergoing mitosis? ii) do 2A-expressing cells undergo apoptotic cell death due to an increased burden of genomic lesions?

5.3 Resistance to cancer therapeutics

In breast cancer, it has been estimated that mutations leading to constitutive activation of the PI3K-AKT pathway occur in more than 70% of cases [150]. While PI3K inhibitors properly block PI3K-AKT signaling in PI3Ki-(BYL719) sensitive cell lines, these tumors eventually become refractory to the treatment [151]. When BYL719-sensitive cell lines

were selected for resistance, the resistant clones had reactivated mTORC1 evidenced by hyperphosphorylated RPS6 (ribosomal protein S6) – a marker for S6K1 activity and indirect readout of mTORC1 signaling. Treatment with a Rapamycin analog was sufficient to sensitize the resistant cells to BYL719, and the combined treatment halted xenograft tumor growth [152].

In melanoma, the RAF protein is the driver oncogene in at least 50% of cases resulting in persistent activation of the MEK-ERK-RSK pathway [153, 154]. Despite excellent advances in the development of RAF and MEK inhibitors and robust initial responses to these agents, patients eventually relapse [155, 156]. In xenograft tumor models and patient biopsies, mTORC1 activity was positively correlated with resistance to the treatment [157]. Interestingly, sustained RPS6 phosphorylation was associated with poor prognosis, and initial responders that became refractory to the treatment showed a reappearance of RPS6 phosphorylation in tumors.

In human non-small lung cancer, 15% of patients carry activating mutations in the kinase domain of EGFR (epidermal growth factor receptor), a member in the RTK family of receptors [157, 158]. In-frame deletions in exon 19 and the L858R mutation account for 85% of all oncogenic EGFR mutations and confer sensitivity to the tyrosine kinase inhibitors (TKIs) erlotinib and gefitinib. Despite multiple clinical trials showing robust initial response rates of EGFR-mutant tumors to TKIs, acquired resistance emerges in most cases [64]. In cell lines that develop tolerance to long-term treatment, EGFR and ERK1/2 are efficiently inhibited, but RPS6 phosphorylation rebounds [159]. Furthermore, in genetically engineered mice harboring EGFR mutations with acquired resistance to the treatment, EGFR and ERK1/2 inhibition was persistent in the majority of resistance nodules, whereas RPS6 phosphorylation would reappear in more than 70% of the cases [159]. Rapamycin treatment could overcome this resistance in both xenograft and EGFR mutant mouse models [160]. Importantly, no genetic lesions known to increase mTORC1 activation, e.g., PTEN, AKT1, TSC1, TSC2, PI3KCA, were detected in these tumors, raising the possibility that acquired resistance to EGFRi could indeed be due to compensatory over-activation of the mTOR pathway [159].

While mutations that enhance Rag GTPase signaling to mTORC1 or activating mutations on mTOR itself have been identified, most oncogenes and tumor suppressors that regulate mTORC1 activity do so through the TSC complex [126, 157]. As a result, it is likely that aberrant inhibition of the TSC complex due to disruptions in upstream signaling pathways commonly leads to sustained mTORC1 activation, contributing to therapeutic resistance. To investigate the involvement of TSC1 phosphorylation in drug resistance, it would be tempting to deploy a panel of cell lines known to harbor mutations in the PI3K-AKT or RAS pathways similar to what was described above. Cultured cells will be subjected to an established first-line treatment for the respective malignancy and selected for the appearance of drug-resistant clones that are reported to manifest for a given cell line [159, 161]. During this process, a thorough inspection of mTORC1 signaling coupled to TSC1 protein levels and TSC complex localization dynamics would provide evidence as to whether the resurgence in mTORC1 activity in tumors displaying acquired tolerance to the treatment can be ascribed to the signaling events on TSC1 and the TSC-TFEB axis.

6 Materials and methods

6.1 Cell culture

HEK293FT, U2OS, and MEF cells were grown in high-glucose Dulbecco's modified Eagle's medium (DMEM) (#41965-039, Gibco) supplemented with 10% fetal bovine serum and 1x Penicillin-Streptomycin (#15140-122, Gibco) at 37°C with 5% CO_2. The identity of the HEK293FT cells was validated by the Multiplex human Cell Line Authentication test (Multiplexion GmbH), which uses a SNP (single nucleotide polymorphism) typing approach and was performed as described at www.multiplexion.de. All cell lines were routinely tested for Mycoplasma contamination using a PCR-based approach and were confirmed to be Mycoplasma-free.

6.2 Cell culture treatments

For AA starvation, custom-made starvation media was formulated according to the Gibco recipe for high-glucose DMEM (Table 1), omitting all AAs. The lists of components used for the starvation media are summarized in Table 2. The media was filtered through a 0.22 µm filter device and tested for proper pH (pH 7.4) and osmolality before use. For the respective AA-replete treatment, commercially available high-glucose DMEM media supplemented with 10% fetal bovine serum and 1x Penicillin-Streptomycin was used. All treatment media were supplemented with 10% dFBS (dialyzed FBS) and 1x P/S. For this purpose, FBS was dialyzed against 1x PBS (phosphate-buffered saline) through a 3,500 MWCO (molecular weight cut-off) dialysis tubing to remove all AAs that FBS might contain. For amino-acid starvation, culture media was replaced with starvation media for one hour. For AA add-back experiments, cells were first starved as described above, and then starvation media was replaced with high-glucose DMEM supplemented with 10% fetal bovine serum and 1x Penicillin-Streptomycin media for 30 minutes. For glucose starvation, cells were cultured for 16 hours in DMEM without Glucose (#11966025, Gibco) supplemented with 10% dFBS and 1x P/S. For glucose add-back, cells were first starved for glucose as described, and media was replaced with high-glucose DMEM supplemented with 10% fetal bovine serum and 1x Penicillin-Streptomycin for 2 hours. For growth factor starvation,

cells were cultured for 16 hours in high-glucose DMEM supplemented with 1x P/S, without FBS. For growth factor add-back, FBS was added drop-wise to the cells at 10% final concentration for 10 minutes. For Bafilomycin A1 treatment (#BML-CM110-0100, Enzo), the drug was added to a final concentration of 100 nM for 8 hours. Torin1 (#4247, Tocris Bioscience) was added to a final concentration of 250 nM for 1 hour. Rapamycin (#S1039; Selleckchem) was added to a final concentration of 20 nM, as indicated in the figure legends. MG132 (#M7449, Sigma) was added to a final concentration of 10 μM for 8 hours. Cycloheximide (#239763, Sigma) was added to a final concentration of 100 μM as indicated in the figure legends.

Table 1. **Inorganic components and amino acids used for the preparation of custom-made media.**

Inorganic compounds

Supplier	Name	Catalog number
Applichem	CaCl2-2H20	A1873
Sigma	Iron(III) nitrate nonahydrate	F8508
Sigma	Magnesium sulfateheptahydrate	13142
Roth	Potassium Chloride	6781.1
Sigma	Sodium bicarbonate	S5761
Sigma	Sodium chloride	31434
Roth	Sodium dihydrogen phosphate monohydrate	K300.2
Applichem	D-Glucose	A1422

Amino acids

Sigma	L-Arginine	A8094
Sigma	L-Cystin	30200
Sigma	L-Glutamine	49419
Sigma	L-Histidine	H8000
Sigma	L-Leucine	L8912
Sigma	L-Lysine HCl	L5626
Sigma	L-Methionine	M9625
Sigma	L-Phenylalanine	P5482

Sigma	L-Proline	P0380
Alfa Aesar	L-Serine	J62187
Sigma	L-Threonine	T8625
Sigma	L-Tryptophan	T0254
Applichem	L-Tyrosine	A1677
Sigma	L-Valine	V0500

6.3 Generation of knockout cell lines

The HEK293FT TSC1 and TSC2 knockout cell lines were generated using the pX459-based CRISPR/Cas9 method, as described elsewhere[51]. The sgRNA expression vectors were generated by cloning appropriate DNA oligonucleotides into the BbsI restriction sites of the pX459 vector (#62988, Addgene). An empty pX459 vector was used to generate matching control cell lines. In brief, transfected cells were selected with 3 µg/mL puromycin (#A1113803, Gibco) 36-40 hours post-transfection. Single-cell clones were generated by FACS-sorting into 96-well plates, and knockout clones were validated by immunoblotting and functional assays. The oligonucleotide sequences used for the generation of knockout cell lines are listed below.

Table 2. Oligonucleotide sequence of single-guide RNAs.

Target Gene	Oligonucleotide sequence
TSC1-gRNA-exon3-s	CACCGGGCCCAACAAGCAAATGTCG
TSC1-gRNA-exon3-as	AAACCGACATTTGCTTGTTGGGCCC
TSC2-gRNA-exon2-s	CACCGGACGGAGTTTATCATCACCG
TSC2-gRNA-exon2-as	AAACCGGTGATGATAAACTCCGTCC

6.4 Generation of stable cell lines

The polyclonal reconstituted HEK293FT TSC2 KO cell lines stably expressing TSC2-WT or -N1643K GAP inactive mutant were generated using a doxycycline-inducible sleeping-beauty-based transposon system [162, 163]. In brief, TSC2 KO cells were co-transfected with pITR-TSC2WT or pITR-TSC2N1643K and the transposase-expressing pCMV-Trp vector in a 10:1 ratio. Forty hours post-transfection, cells were selected with 3 µg/mL puromycin (#A1113803, Gibco). The polyclonal cell lines were subsequently maintained in media containing the selection agent. Doxycycline-

induced expression from the integrated plasmid was tested by treating the cells overnight with 1 µg/mL doxycycline (#D9891, Sigma). For experiments, all cell lines were used without doxycycline induction to allow for low-level, leaky TSC2 expression.

6.5 Cell lysis and immunoblotting

For standard SDS-PAGE and immunoblotting experiments, cells were lysed in ice-cold Triton lysis buffer (50 mM Tris pH 7.5, 1% Triton X-100, 150 mM NaCl, 50 mM NaF, 2 mM Na-vanadate, 10 mM beta-glycerophosphate), supplemented with 1x PhosSTOP phosphatase inhibitors (#04906837001, Roche) and 1x cOmplete protease inhibitors (#11697498001, Roche), for 10 minutes on ice. For dephosphorylation studies, cells were lysed in Triton lysis buffer without phosphatase inhibitors and EDTA. Lysates were incubated in the presence of lambda PP and $MnCl_2$ (10 mM) for 30 minutes at 30°C. Lysates were clarified by centrifugation (14,000 rcf, 10 min, 4°C), and supernatants were transferred to a new tube. Protein concentration was determined using a Protein Assay Dye Reagent (#5000006, Bio-Rad). Normalized samples were boiled in 1x SDS sample buffer for 5 min at 95°C (6x SDS sample buffer: 350 mM Tris-HCl pH 6.8, 30% glycerol, 600 mM DTT, 12% SDS, 0.12% bromophenol blue). Protein samples were subjected to electrophoretic separation on SDS-PAGE and analyzed by standard Western blotting techniques. In brief, proteins were transferred to nitrocellulose membranes (#10600002 or #10600001, Amersham) and stained with 0.2% Ponceau solution (#33427-01, Serva) to confirm equal loading. Membranes were blocked with 5% skim milk powder (#42590, Serva) in TBS-T 1x TBS, 0.1% Tween-20 (#A1389, AppliChem) for 1 hour at room temperature, washed three times for 5 min with TBS-T and then incubated with primary antibodies in TBS-T, 2% bovine serum albumin (BSA; #10735086001, Roche; #8076, Carl Roth) overnight at 4°C. The next day, membranes were washed three times for 5 min with TBS-T and incubated with the appropriate HRP-conjugated secondary antibodies (1:10000 in 5% milk in TBS-T) for 1 hour at room temperature. Signals were detected by enhanced chemiluminescence (ECL), using ECL Western Blotting Substrate (#W1015, Promega) or SuperSignal West Femto Substrate (#34095, Thermo Scientific) for weaker signals. Immunoblot images were captured on films (#28906835, GE Healthcare; #4741019289, Fujifilm). Blots were scanned and then quantified using

GelAnalyzer 19.1. A list of all primary and secondary antibodies used in this study is provided in Table 3 and the respective section of the key resources table.

Table 3. Antibodies used in co-IP/IP, Western blot, and IVK assay experiments.

Antibody	Dilution	Supplier	Catalog Number
phospho-p70 S6 Kinase (Thr389) (D5U1O) Rabbit monoclonal	1:1,000	Cell Signaling Technology	97596
S6 Kinase Rabbit polyclonal	1:1,000	Cell Signaling Technology	9202
phospho-TFEB (Ser122) (E9M5M) Rabbit monoclonal	1:1,000	Cell Signaling Technology	87932
TFEB Rabbit polyclonal	1:1,000	Cell Signaling Technology	4240
Phospho-AKT (Thr308) (D25E6) Rabbit monoclonal	1:500	Cell Signaling Technology	13038
phospho-AKT (Ser473) Rabbit polyclonal	1:1,000	Cell Signaling Technology	9271
phospho-4E-BP1 (Ser65) (D9G1Q) Rabbit monoclonal	1:1,000	Cell Signaling Technology	13443
phospho-4E-BP1 (Thr37/46) Rabbit polyclonal	1:1,000	Cell Signaling Technology	9459
TSC1 (D43E2) Rabbit monoclonal	1:1,000	Cell Signaling Technology	6935

TSC1 Rabbit polyclonal	1:1,000	Bethyl Laboratories	A300-316A
TSC2 Rabbit polyclonal	1:5,000	Cell Signaling Technology	4308
phospho-RAPTOR (Ser792)	1:1,000	Cell Signaling Technology	2083
RAPTOR (24C12) Rabbit monoclonal	1:1,000	Cell Signaling Technology	2280
RICTOR (D16H) Rabbit monoclonal	1:1,000	Cell Signaling Technology	9476
RagA (D8B5) Rabbit monoclonal	1:1,000	Cell Signaling Technology	4357
RagB (D18F3) Rabbit monoclonal	1:1,000	Cell Signaling Technology	8150
RagC (D8H5) Rabbit monoclonal	1:1,000	Cell Signaling Technology	9480
RagD Rabbit polyclonal	1:1,000	Cell Signaling Technology	4470
phospho- threonine-proline Mouse monoclonal	1:500	Cell Signaling Technology	9391
GAPDH (14C10) Rabbit monoclonal	1:5,000	Cell Signaling Technology	2118
FLAG Rabbit polyclonal	1:1,000	Cell Signaling Technology	2368
HA (3F10) Rat monoclonal	1:3,000	Roche	11867423001

6.6 Immunoprecipitation (co-IP/IP)

For co-immunoprecipitation experiments, cells were lysed in CHAPS IP buffer (50 mM Tris pH 7.5, 0.3% CHAPS, 150 mM NaCl, 50 mM NaF, 2 mM Na-vanadate, 10 mM beta-glycerophosphate) supplemented with 1x PhosSTOP phosphatase inhibitors

(#04906837001, Roche) and 1x cOmplete protease inhibitors (#11697498001, Roche) for 10 minutes on ice. For TSC1-IP experiments all procedures were carried out similarly to the co-IP protocol, with using Triton-X100 1% instead of CHAPS 0.3% in the lysis buffer, being the only exception. Samples were clarified by centrifugation (14000 rcf, 10 min, 4°C), and a portion of the samples was taken as input. For epitope tagged-IPs, 40 µL of pre-equilibrated HA- (#A2095, Sigma) or FLAG-conjugated agarose beads (#A2095, Sigma) were added to the remaining volume of the supernatants and the IP samples were incubated at 4°C on a rotating mixer for 2 hours. For endogenous protein IPs, the remaining volume of the supernatants was incubated with 1-2 µl of antibody at 4°C on an overhead rotator over-night, followed by incubation with 40 µl pre-equilibrated Protein A agarose beads (#11134515001, Roche) for an additional hour at 4°C on an overhead rotator. For all IPs, beads were then washed three times with CHAPS IP wash buffer (50 mM Tris pH 7.5, 0.3% CHAPS, 150 mM NaCl, 50 mM NaF, 1 mM EDTA) and boiled in 2x SDS loading buffer. Samples were analyzed by SDS-PAGE, and the presence of co-immunoprecipitated proteins was detected by immunoblotting with appropriate specific antibodies.

6.7 Sample preparation for mass-spectrometry

To prepare the IP fractions for mass spectrometry, after washing the beads in IP wash buffer, immobilized proteins were washed thrice in Tris 50 mM pH 7.5 and eluted in 100 µL of elution buffer (5 ng/µL, 50mM Tris pH7.5 and 1mM TCEP (Tris (2-carboxyethyl) phosphine), and 5mM CAA (chloroacetamide). Immobilized proteins were incubated in elution buffer for 1 hour at room temperature. After incubation, the supernatants were transferred to 0.5 mL tubes and incubated at 37°C overnight to ensure complete tryptic digestion. Digestion was stopped by adding 50% FA to the reaction at a final concentration of 1%. Samples were centrifuged at 20,000 g for 10 min at RT and supernatants were collected. C-18-SD StageTips were washed and equilibrated sequentially with 200 µL methanol, 200 µL 40% ACN (acetonitrile)/0.1% FA (formic acid) and 200 µL 0.1% FA by centrifugation, each step for 1 min at RT. Samples were diluted with 0.1% FA, loaded in StageTips and centrifuged for 1–2 min at RT. StageTips were then washed twice with 200 µL 0.1% FA. Tryptic peptides were eluted from StageTips with 100 µL 40% acetonitrile (ACN)/0.1% formic acid (FA) by

centrifugation (300 g, 4 min, RT). Eluates were dried in a Speed-Vac at 45°C for 1 hour and resuspended in 20 µL 0.1% FA. Peptides were stored at -20°C until subjection to LC-MS/MS analysis.

6.8 Gene silencing experiments

Transient knockdown of LAMTOR1, RAGA, and RAGC was performed using 20 nM of 4 siGENOME gene-specific siRNAs (Horizon Discoveries). A siRNA duplex targeting the *R. reniformis* luciferase gene (RLuc) (#P-002070-01-50, Horizon Discoveries) was used as a control. Transfections were performed using Lipofectamine RNAiMAX reagent (13778075, Invitrogen). The RNAi sequences for knockdown experiments are listed below.

6.9 RNA isolation and cDNA synthesis

RNA was isolated from HEK293FT cells using standard TRIzol/chloroform-based extraction (#15596018, Thermo Fisher Scientific), according to the manufacturer's instructions. For cDNA synthesis, 2 µg of RNA was transcribed to cDNA using the RevertAid H Minus Reverse Transcriptase kit (#EP0451, Thermo Fisher Scientific) according to the manufacturer's instructions.

6.10 Plasmid transfections

The majority of Plasmid DNA transfections in HEK293FT cells were performed using Effectene transfection reagent (#301425, QIAGEN), according to the manufacturer's instructions, except for the HA-RAPTOR co-IP experiments and the transient expression of TSC1-2A mutant in which case X-tremeGENE HP (6366236001, Roche) transfection reagent was used. For plasmid transfections in MEFs, the ViaFect Transfection Reagent was used (#E4981, Promega), according to the manufacturer's instructions. U2OS were transfected with X-tremeGENE HP.

6.11 Plasmids and molecular cloning

Full-length human TSC1 (Accession NM_000365) was sub-cloned from a pRK7-FLAG-TSC1 plasmid into a pITR-TTP-bsd vector [164] using SfiI and NotI restriction sites. Site-directed mutagenesis for generating the T1047A and S1080A substitutions in the TSC1-2A mutant was performed using overlap PCR (see table below for mutagenic oligonucleotide sequences). The PRK7-FLAG-TSC1 and pcDNA3-FLAG-

TSC2 vectors were a kind gift of Brendan Manning (Addgene plasmid #8995, Addgene plasmid #14129). The pcDNA3-FLAG-TSC2 plasmid was a kind gift of Brendan Manning (Addgene plasmid, #14129). The N1643K GAP inactive mutant in TSC2 was generated with TOPO cloning and inserted into the pcDNA3-FLAG-TSC2 plasmid using the Bsu36I and EcoRV restriction sites (see table below for mutagenic oligonucleotide sequences). The TSC2-expressing construct lacking the 424 N-terminal amino acid residues (425-1784) has been described previously [67]. Full-length human RHEB was subcloned from a pRK5-HA-GST-RHEB plasmid into a pcDNA3-FLAG vector using EcoRI and NotI restriction sites. The pRK5-HA-GST-RHEB and pRK5-HA-RAPTOR plasmids were a kind gift of David Sabatini (Addgene plasmid #14951, #8513). Active and inactive RHEB mutants were generated using site-directed mutagenesis. All cloning and mutagenesis procedures were performed using Phusion High-Fidelity DNA Polymerase (M0530L, NEB).

Table 4. Mutagenic oligonucleotide sequences used in molecular cloning.

Target	Oligonucleotide sequence
TSC1-T1047A-s	AGCAGCGAGCTTTCTGCCCCAGAGAAAC
TSC1-T1047A-as	GTTTCTCTGGGGCAGAAAGCTCGCTGCT
TSC1-S1080A-s	CTGTGGGCGCACTTCCCAG
TSC1-S1080A-as	CTGGGAAGTGCGCCCACAG
TSC2-N1643K-s	GCGCCACCTGGGCAAGGACTTTGTGTCCATTG
TSC2-N1643K-as	CAATGGACACAAAGTCCTTGCCCAGGTGGCGC
RHEB-S16H-s	GAAGAATTCATGCCGCAGTCCAAGTCCCGGAAGATCGCGATCC TGGGCTACCGGcaTGTGGGGAAATCC
RHEB-I39K-s	CTACGATCCAACCAAAGAAAACACTT
RHEB-I39K-as	AAGTGTTTTCTTTGGTTGGATCGTAG

6.12 mTOR kinase activity assay

Cells of a near-confluent 10-cm dish were lysed in CHAPS IP buffer for 10 minutes on ice. Samples were clarified by centrifugation (14,000 rcf, 10 minutes, 4 °C), supernatants were collected, and a portion was kept as input material. The remaining volume of the supernatants was used for immunoprecipitation by incubation with 2 µL

of anti-mTOR antibody (see antibody table) over-night on an overhead rotator at 4 °C, followed by incubation with 40 µL of pre-equilibrated Protein A agarose bead for an additional hour rotating at 4°C. Beads were then washed three times with IP wash buffer and once with kinase wash buffer (25 mM HEPES pH 7.4 (#A3724, Applichem), 20 mM KCl (#6878.1, Roth). Kinase reactions were prepared by adding 10 µL 3x kinase assay buffer (75 mM HEPES/KOH pH 7.4 (#60377, Sigma), 60 mM KCl, 30 mM MgCl2 (#1.058.330.250, Merck)) to the beads. Reactions were started by adding 10 µL of kinase assay start buffer (25 mM HEPES/KOH pH 7.4, 140 mM KCl, 10 mM MgCl2), supplemented with 500 µM ATP and 35 ng of recombinant His-4E-BP1 or 50 ng of His-TSC1 substrate. All reactions were incubated at 30°C for 30 minutes and stopped by the addition of 2x SDS sample buffer, followed by boiling for 5 minutes at 95°C. Samples were resolved by SDS-PAGE.

6.13 Recombinant protein expression

E. coli BL21 RP electrocompetent bacteria were transformed with a pETM11 vector coding for His-4E-BP1 or His-TSC1 (989-1163). Protein expression was induced with isopropyl-β-D-thiogalactopyranoside (IPTG); #A1008, Applichem) for four hours at 37°C. Expressed proteins were immobilized on Ni-NTA agarose beads and eluted in 250 mM imidazole.

6.14 Statistical analysis

Statistical analysis and presentation of quantification data were performed using GraphPad Prism (versions 9 and 10). All relevant information on the statistical details of experiments is provided in the figure legends. Data in all graphs are shown as mean ± SD. Significance for S6K1 and TFEB phosphorylation for the indicated pairwise comparisons was calculated using one-way ANOVA with *post hoc* Tukey's multiple comparisons test. Significance for TSC1 protein levels in response to CHX ± Torin1 treatment was calculated using one-way ANOVA with Uncorrected Fisher's LSD test.

7 References

1. Vezina, C., A. Kudelski, and S.N. Sehgal, *Rapamycin (AY-22,989), a new antifungal antibiotic. I. Taxonomy of the producing streptomycete and isolation of the active principle.* J Antibiot (Tokyo), 1975. **28**(10): p. 721-6.
2. Heitman, J., N.R. Movva, and M.N. Hall, *Targets for cell cycle arrest by the immunosuppressant rapamycin in yeast.* Science, 1991. **253**(5022): p. 905-9.
3. Kunz, J., et al., *Target of rapamycin in yeast, TOR2, is an essential phosphatidylinositol kinase homolog required for G1 progression.* Cell, 1993. **73**(3): p. 585-96.
4. Cafferkey, R., et al., *Dominant missense mutations in a novel yeast protein related to mammalian phosphatidylinositol 3-kinase and VPS34 abrogate rapamycin cytotoxicity.* Mol Cell Biol, 1993. **13**(10): p. 6012-23.
5. Brown, E.J., et al., *A mammalian protein targeted by G1-arresting rapamycin-receptor complex.* Nature, 1994. **369**(6483): p. 756-8.
6. Sabatini, D.M., et al., *RAFT1: a mammalian protein that binds to FKBP12 in a rapamycin-dependent fashion and is homologous to yeast TORs.* Cell, 1994. **78**(1): p. 35-43.
7. Sabers, C.J., et al., *Isolation of a protein target of the FKBP12-rapamycin complex in mammalian cells.* J Biol Chem, 1995. **270**(2): p. 815-22.
8. Liu, G.Y. and D.M. Sabatini, *mTOR at the nexus of nutrition, growth, ageing and disease.* Nat Rev Mol Cell Biol, 2020. **21**(4): p. 183-203.
9. Benjamin, D., et al., *Rapamycin passes the torch: a new generation of mTOR inhibitors.* Nat Rev Drug Discov, 2011. **10**(11): p. 868-80.
10. Aylett, C.H., et al., *Architecture of human mTOR complex 1.* Science, 2016. **351**(6268): p. 48-52.
11. Yang, H., et al., *mTOR kinase structure, mechanism and regulation.* Nature, 2013. **497**(7448): p. 217-23.
12. Yang, H., et al., *Mechanisms of mTORC1 activation by RHEB and inhibition by PRAS40.* Nature, 2017. **552**(7685): p. 368-373.
13. Schalm, S.S. and J. Blenis, *Identification of a conserved motif required for mTOR signaling.* Curr Biol, 2002. **12**(8): p. 632-9.
14. Sancak, Y., et al., *The Rag GTPases bind raptor and mediate amino acid signaling to mTORC1.* Science, 2008. **320**(5882): p. 1496-501.
15. Kim, E., et al., *Regulation of TORC1 by Rag GTPases in nutrient response.* Nat Cell Biol, 2008. **10**(8): p. 935-45.
16. Sarbassov, D.D., et al., *Prolonged rapamycin treatment inhibits mTORC2 assembly and Akt/PKB.* Mol Cell, 2006. **22**(2): p. 159-68.
17. Goul, C., R. Peruzzo, and R. Zoncu, *The molecular basis of nutrient sensing and signalling by mTORC1 in metabolism regulation and disease.* Nat Rev Mol Cell Biol, 2023. **24**(12): p. 857-875.
18. Ma, X.M. and J. Blenis, *Molecular mechanisms of mTOR-mediated translational control.* Nat Rev Mol Cell Biol, 2009. **10**(5): p. 307-18.
19. Raught, B., et al., *Phosphorylation of eucaryotic translation initiation factor 4B Ser422 is modulated by S6 kinases.* EMBO J, 2004. **23**(8): p. 1761-9.

20. Holz, M.K., et al., *mTOR and S6K1 mediate assembly of the translation preinitiation complex through dynamic protein interchange and ordered phosphorylation events.* Cell, 2005. **123**(4): p. 569-80.
21. Shahbazian, D., et al., *The mTOR/PI3K and MAPK pathways converge on eIF4B to control its phosphorylation and activity.* EMBO J, 2006. **25**(12): p. 2781-91.
22. Dorrello, N.V., et al., *S6K1- and betaTRCP-mediated degradation of PDCD4 promotes protein translation and cell growth.* Science, 2006. **314**(5798): p. 467-71.
23. Yang, H.S., et al., *The transformation suppressor Pdcd4 is a novel eukaryotic translation initiation factor 4A binding protein that inhibits translation.* Mol Cell Biol, 2003. **23**(1): p. 26-37.
24. Yang, H.S., et al., *A novel function of the MA-3 domains in transformation and translation suppressor Pdcd4 is essential for its binding to eukaryotic translation initiation factor 4A.* Mol Cell Biol, 2004. **24**(9): p. 3894-906.
25. Choi, K.M., L.P. McMahon, and J.C. Lawrence, Jr., *Two motifs in the translational repressor PHAS-I required for efficient phosphorylation by mammalian target of rapamycin and for recognition by raptor.* J Biol Chem, 2003. **278**(22): p. 19667-73.
26. Nojima, H., et al., *The mammalian target of rapamycin (mTOR) partner, raptor, binds the mTOR substrates p70 S6 kinase and 4E-BP1 through their TOR signaling (TOS) motif.* J Biol Chem, 2003. **278**(18): p. 15461-4.
27. Wang, X., et al., *The C terminus of initiation factor 4E-binding protein 1 contains multiple regulatory features that influence its function and phosphorylation.* Mol Cell Biol, 2003. **23**(5): p. 1546-57.
28. Lahr, R.M., et al., *The La-related protein 1-specific domain repurposes HEAT-like repeats to directly bind a 5'TOP sequence.* Nucleic Acids Res, 2015. **43**(16): p. 8077-88.
29. Fonseca, B.D., et al., *La-related Protein 1 (LARP1) Represses Terminal Oligopyrimidine (TOP) mRNA Translation Downstream of mTOR Complex 1 (mTORC1).* J Biol Chem, 2015. **290**(26): p. 15996-6020.
30. Ganley, I.G., et al., *ULK1.ATG13.FIP200 complex mediates mTOR signaling and is essential for autophagy.* J Biol Chem, 2009. **284**(18): p. 12297-305.
31. Kamada, Y., et al., *Tor directly controls the Atg1 kinase complex to regulate autophagy.* Mol Cell Biol, 2010. **30**(4): p. 1049-58.
32. Hosokawa, N., et al., *Nutrient-dependent mTORC1 association with the ULK1-Atg13-FIP200 complex required for autophagy.* Mol Biol Cell, 2009. **20**(7): p. 1981-91.
33. Park, J.M., et al., *The ULK1 complex mediates MTORC1 signaling to the autophagy initiation machinery via binding and phosphorylating ATG14.* Autophagy, 2016. **12**(3): p. 547-64.
34. Ma, X., et al., *MTORC1-mediated NRBF2 phosphorylation functions as a switch for the class III PtdIns3K and autophagy.* Autophagy, 2017. **13**(3): p. 592-607.
35. Ben-Sahra, I., et al., *mTORC1 induces purine synthesis through control of the mitochondrial tetrahydrofolate cycle.* Science, 2016. **351**(6274): p. 728-733.

36. Hoxhaj, G. and B.D. Manning, *The PI3K-AKT network at the interface of oncogenic signalling and cancer metabolism.* Nat Rev Cancer, 2020. **20**(2): p. 74-88.
37. Valvezan, A.J. and B.D. Manning, *Molecular logic of mTORC1 signalling as a metabolic rheostat.* Nat Metab, 2019. **1**(3): p. 321-333.
38. Ben-Sahra, I., et al., *Stimulation of de novo pyrimidine synthesis by growth signaling through mTOR and S6K1.* Science, 2013. **339**(6125): p. 1323-8.
39. Shimano, H. and R. Sato, *SREBP-regulated lipid metabolism: convergent physiology - divergent pathophysiology.* Nat Rev Endocrinol, 2017. **13**(12): p. 710-730.
40. Peterson, T.R., et al., *mTOR complex 1 regulates lipin 1 localization to control the SREBP pathway.* Cell, 2011. **146**(3): p. 408-20.
41. Duvel, K., et al., *Activation of a metabolic gene regulatory network downstream of mTOR complex 1.* Mol Cell, 2010. **39**(2): p. 171-83.
42. Puertollano, R., et al., *The complex relationship between TFEB transcription factor phosphorylation and subcellular localization.* EMBO J, 2018. **37**(11).
43. Takla, M., S. Keshri, and D.C. Rubinsztein, *The post-translational regulation of transcription factor EB (TFEB) in health and disease.* EMBO Rep, 2023. **24**(11): p. e57574.
44. Pena-Llopis, S., et al., *Regulation of TFEB and V-ATPases by mTORC1.* EMBO J, 2011. **30**(16): p. 3242-58.
45. Martina, J.A., et al., *MTORC1 functions as a transcriptional regulator of autophagy by preventing nuclear transport of TFEB.* Autophagy, 2012. **8**(6): p. 903-14.
46. Settembre, C., et al., *A lysosome-to-nucleus signalling mechanism senses and regulates the lysosome via mTOR and TFEB.* EMBO J, 2012. **31**(5): p. 1095-108.
47. Vega-Rubin-de-Celis, S., et al., *Multistep regulation of TFEB by MTORC1.* Autophagy, 2017. **13**(3): p. 464-472.
48. Roczniak-Ferguson, A., et al., *The transcription factor TFEB links mTORC1 signaling to transcriptional control of lysosome homeostasis.* Sci Signal, 2012. **5**(228): p. ra42.
49. Napolitano, G., et al., *A substrate-specific mTORC1 pathway underlies Birt-Hogg-Dube syndrome.* Nature, 2020. **585**(7826): p. 597-602.
50. Martina, J.A. and R. Puertollano, *Rag GTPases mediate amino acid-dependent recruitment of TFEB and MITF to lysosomes.* J Cell Biol, 2013. **200**(4): p. 475-91.
51. Ran, F.A., et al., *Genome engineering using the CRISPR-Cas9 system.* Nat Protoc, 2013. **8**(11): p. 2281-2308.
52. Gollwitzer, P., et al., *A Rag GTPase dimer code defines the regulation of mTORC1 by amino acids.* Nat Cell Biol, 2022. **24**(9): p. 1394-1406.
53. Cui, Z., et al., *Structure of the lysosomal mTORC1-TFEB-Rag-Ragulator megacomplex.* Nature, 2023. **614**(7948): p. 572-579.
54. Alesi, N., et al., *TFEB drives mTORC1 hyperactivation and kidney disease in Tuberous Sclerosis Complex.* Nat Commun, 2024. **15**(1): p. 406.
55. Hansmann, P., et al., *Structure of the TSC2 GAP Domain: Mechanistic Insight into Catalysis and Pathogenic Mutations.* Structure, 2020. **28**(8): p. 933-942 e4.

56. Yang, H., et al., *Structural insights into TSC complex assembly and GAP activity on Rheb.* Nat Commun, 2021. **12**(1): p. 339.
57. Henske, E.P., et al., *Allelic loss is frequent in tuberous sclerosis kidney lesions but rare in brain lesions.* Am J Hum Genet, 1996. **59**(2): p. 400-6.
58. Hoogeveen-Westerveld, M., et al., *The TSC1-TSC2 complex consists of multiple TSC1 and TSC2 subunits.* BMC Biochem, 2012. **13**: p. 18.
59. Fitzian, K., et al., *TSC1 binding to lysosomal PIPs is required for TSC complex translocation and mTORC1 regulation.* Mol Cell, 2021. **81**(13): p. 2705-2721 e8.
60. Qin, J., et al., *Structural Basis of the Interaction between Tuberous Sclerosis Complex 1 (TSC1) and Tre2-Bub2-Cdc16 Domain Family Member 7 (TBC1D7).* J Biol Chem, 2016. **291**(16): p. 8591-601.
61. Gai, Z., et al., *Structure of the TBC1D7-TSC1 complex reveals that TBC1D7 stabilizes dimerization of the TSC1 C-terminal coiled coil region.* J Mol Cell Biol, 2016. **8**(5): p. 411-425.
62. Garami, A., et al., *Insulin activation of Rheb, a mediator of mTOR/S6K/4E-BP signaling, is inhibited by TSC1 and 2.* Mol Cell, 2003. **11**(6): p. 1457-66.
63. Inoki, K., et al., *Rheb GTPase is a direct target of TSC2 GAP activity and regulates mTOR signaling.* Genes Dev, 2003. **17**(15): p. 1829-34.
64. Chong, C.R. and P.A. Janne, *The quest to overcome resistance to EGFR-targeted therapies in cancer.* Nat Med, 2013. **19**(11): p. 1389-400.
65. Woodford, M.R., et al., *Tumor suppressor Tsc1 is a new Hsp90 co-chaperone that facilitates folding of kinase and non-kinase clients.* EMBO J, 2017. **36**(24): p. 3650-3665.
66. Schrotter, S., et al., *The non-essential TSC complex component TBC1D7 restricts tissue mTORC1 signaling and brain and neuron growth.* Cell Rep, 2022. **39**(7): p. 110824.
67. Demetriades, C., N. Doumpas, and A.A. Teleman, *Regulation of TORC1 in response to amino acid starvation via lysosomal recruitment of TSC2.* Cell, 2014. **156**(4): p. 786-99.
68. Menon, S., et al., *Spatial control of the TSC complex integrates insulin and nutrient regulation of mTORC1 at the lysosome.* Cell, 2014. **156**(4): p. 771-85.
69. Zhang, Y., et al., *Rheb is a direct target of the tuberous sclerosis tumour suppressor proteins.* Nat Cell Biol, 2003. **5**(6): p. 578-81.
70. Tee, A.R., et al., *Tuberous sclerosis complex gene products, Tuberin and Hamartin, control mTOR signaling by acting as a GTPase-activating protein complex toward Rheb.* Curr Biol, 2003. **13**(15): p. 1259-68.
71. Yu, Y., et al., *Structural basis for the unique biological function of small GTPase RHEB.* J Biol Chem, 2005. **280**(17): p. 17093-100.
72. Buerger, C., B. DeVries, and V. Stambolic, *Localization of Rheb to the endomembrane is critical for its signaling function.* Biochem Biophys Res Commun, 2006. **344**(3): p. 869-80.
73. Hao, F., et al., *Rheb localized on the Golgi membrane activates lysosome-localized mTORC1 at the Golgi-lysosome contact site.* J Cell Sci, 2018. **131**(3).
74. Thomas, J.D., et al., *Rab1A is an mTORC1 activator and a colorectal oncogene.* Cancer Cell, 2014. **26**(5): p. 754-69.

75. Angarola, B. and S.M. Ferguson, *Weak membrane interactions allow Rheb to activate mTORC1 signaling without major lysosome enrichment.* Mol Biol Cell, 2019. **30**(22): p. 2750-2760.
76. Jia, L., et al., *Rheb-regulated mitochondrial pyruvate metabolism of Schwann cells linked to axon stability.* Dev Cell, 2021. **56**(21): p. 2980-2994 e6.
77. Yang, W., et al., *Rheb mediates neuronal-activity-induced mitochondrial energetics through mTORC1-independent PDH activation.* Dev Cell, 2021. **56**(6): p. 811-825 e6.
78. Melser, S., et al., *Rheb regulates mitophagy induced by mitochondrial energetic status.* Cell Metab, 2013. **17**(5): p. 719-30.
79. Gonzalez, A., et al., *AMPK and TOR: The Yin and Yang of Cellular Nutrient Sensing and Growth Control.* Cell Metab, 2020. **31**(3): p. 472-492.
80. Guertin, D.A., et al., *Ablation in mice of the mTORC components raptor, rictor, or mLST8 reveals that mTORC2 is required for signaling to Akt-FOXO and PKCalpha, but not S6K1.* Dev Cell, 2006. **11**(6): p. 859-71.
81. Inoki, K., et al., *TSC2 is phosphorylated and inhibited by Akt and suppresses mTOR signalling.* Nat Cell Biol, 2002. **4**(9): p. 648-57.
82. Cai, S.L., et al., *Activity of TSC2 is inhibited by AKT-mediated phosphorylation and membrane partitioning.* J Cell Biol, 2006. **173**(2): p. 279-89.
83. Vander Haar, E., et al., *Insulin signalling to mTOR mediated by the Akt/PKB substrate PRAS40.* Nat Cell Biol, 2007. **9**(3): p. 316-23.
84. Sancak, Y., et al., *PRAS40 is an insulin-regulated inhibitor of the mTORC1 protein kinase.* Mol Cell, 2007. **25**(6): p. 903-15.
85. Mendoza, M.C., E.E. Er, and J. Blenis, *The Ras-ERK and PI3K-mTOR pathways: cross-talk and compensation.* Trends Biochem Sci, 2011. **36**(6): p. 320-8.
86. Kodaki, T., et al., *The activation of phosphatidylinositol 3-kinase by Ras.* Curr Biol, 1994. **4**(9): p. 798-806.
87. Suire, S., P. Hawkins, and L. Stephens, *Activation of phosphoinositide 3-kinase gamma by Ras.* Curr Biol, 2002. **12**(13): p. 1068-75.
88. Rodriguez-Viciana, P., et al., *Phosphatidylinositol-3-OH kinase as a direct target of Ras.* Nature, 1994. **370**(6490): p. 527-32.
89. Ma, L., et al., *Phosphorylation and functional inactivation of TSC2 by Erk implications for tuberous sclerosis and cancer pathogenesis.* Cell, 2005. **121**(2): p. 179-93.
90. Roux, P.P., et al., *Tumor-promoting phorbol esters and activated Ras inactivate the tuberous sclerosis tumor suppressor complex via p90 ribosomal S6 kinase.* Proc Natl Acad Sci U S A, 2004. **101**(37): p. 13489-94.
91. Carriere, A., et al., *Oncogenic MAPK signaling stimulates mTORC1 activity by promoting RSK-mediated raptor phosphorylation.* Curr Biol, 2008. **18**(17): p. 1269-77.
92. Wolfson, R.L. and D.M. Sabatini, *The Dawn of the Age of Amino Acid Sensors for the mTORC1 Pathway.* Cell Metab, 2017. **26**(2): p. 301-309.
93. Bar-Peled, L., et al., *Ragulator is a GEF for the Rag GTPases that signal amino acid levels to mTORC1.* Cell, 2012. **150**(6): p. 1196-208.
94. Zhang, T., et al., *Structural basis for Ragulator functioning as a scaffold in membrane-anchoring of Rag GTPases and mTORC1.* Nat Commun, 2017. **8**(1): p. 1394.

95. Su, M.Y., et al., *Hybrid Structure of the RagA/C-Ragulator mTORC1 Activation Complex.* Mol Cell, 2017. **68**(5): p. 835-846 e3.
96. de Araujo, M.E.G., et al., *Crystal structure of the human lysosomal mTORC1 scaffold complex and its impact on signaling.* Science, 2017. **358**(6361): p. 377-381.
97. Rogala, K.B., et al., *Structural basis for the docking of mTORC1 on the lysosomal surface.* Science, 2019. **366**(6464): p. 468-475.
98. Anandapadamanaban, M., et al., *Architecture of human Rag GTPase heterodimers and their complex with mTORC1.* Science, 2019. **366**(6462): p. 203-210.
99. Shen, K., et al., *Architecture of the human GATOR1 and GATOR1-Rag GTPases complexes.* Nature, 2018. **556**(7699): p. 64-69.
100. Wolfson, R.L., et al., *Sestrin2 is a leucine sensor for the mTORC1 pathway.* Science, 2016. **351**(6268): p. 43-8.
101. Valenstein, M.L., et al., *Structure of the nutrient-sensing hub GATOR2.* Nature, 2022. **607**(7919): p. 610-616.
102. Shen, K. and D.M. Sabatini, *Ragulator and SLC38A9 activate the Rag GTPases through noncanonical GEF mechanisms.* Proc Natl Acad Sci U S A, 2018. **115**(38): p. 9545-9550.
103. Lawrence, R.E., et al., *Structural mechanism of a Rag GTPase activation checkpoint by the lysosomal folliculin complex.* Science, 2019. **366**(6468): p. 971-977.
104. Jiang, C., et al., *Ring domains are essential for GATOR2-dependent mTORC1 activation.* Mol Cell, 2023. **83**(1): p. 74-89 e9.
105. Chantranupong, L., et al., *The CASTOR Proteins Are Arginine Sensors for the mTORC1 Pathway.* Cell, 2016. **165**(1): p. 153-164.
106. Wang, S., et al., *Metabolism. Lysosomal amino acid transporter SLC38A9 signals arginine sufficiency to mTORC1.* Science, 2015. **347**(6218): p. 188-94.
107. Rebsamen, M., et al., *SLC38A9 is a component of the lysosomal amino acid sensing machinery that controls mTORC1.* Nature, 2015. **519**(7544): p. 477-81.
108. Chen, J., et al., *SAR1B senses leucine levels to regulate mTORC1 signalling.* Nature, 2021. **596**(7871): p. 281-284.
109. Wyant, G.A., et al., *mTORC1 Activator SLC38A9 Is Required to Efflux Essential Amino Acids from Lysosomes and Use Protein as a Nutrient.* Cell, 2017. **171**(3): p. 642-654 e12.
110. Gu, X., et al., *SAMTOR is an S-adenosylmethionine sensor for the mTORC1 pathway.* Science, 2017. **358**(6364): p. 813-818.
111. Tang, X., et al., *Molecular mechanism of S-adenosylmethionine sensing by SAMTOR in mTORC1 signaling.* Sci Adv, 2022. **8**(26): p. eabn3868.
112. Fernandes, S.A. and C. Demetriades, *The Multifaceted Role of Nutrient Sensing and mTORC1 Signaling in Physiology and Aging.* Front Aging, 2021. **2**: p. 707372.
113. Efeyan, A., et al., *Regulation of mTORC1 by the Rag GTPases is necessary for neonatal autophagy and survival.* Nature, 2013. **493**(7434): p. 679-83.
114. Dai, X., et al., *AMPK-dependent phosphorylation of the GATOR2 component WDR24 suppresses glucose-mediated mTORC1 activation.* Nat Metab, 2023. **5**(2): p. 265-276.

115. Malik, N., et al., *Induction of lysosomal and mitochondrial biogenesis by AMPK phosphorylation of FNIP1.* Science, 2023. **380**(6642): p. eabj5559.
116. Gwinn, D.M., et al., *AMPK phosphorylation of raptor mediates a metabolic checkpoint.* Mol Cell, 2008. **30**(2): p. 214-26.
117. Shaw, R.J., et al., *The LKB1 tumor suppressor negatively regulates mTOR signaling.* Cancer Cell, 2004. **6**(1): p. 91-9.
118. Inoki, K., T. Zhu, and K.L. Guan, *TSC2 mediates cellular energy response to control cell growth and survival.* Cell, 2003. **115**(5): p. 577-90.
119. Yuan, H.X. and K.L. Guan, *The SIN1-PH Domain Connects mTORC2 to PI3K.* Cancer Discov, 2015. **5**(11): p. 1127-9.
120. Cohen, D., et al., *The potential role of custody facilities in controlling sexually transmitted diseases.* Am J Public Health, 1992. **82**(4): p. 552-6.
121. Sarbassov, D.D., et al., *Rictor, a novel binding partner of mTOR, defines a rapamycin-insensitive and raptor-independent pathway that regulates the cytoskeleton.* Curr Biol, 2004. **14**(14): p. 1296-302.
122. Sarbassov, D.D., et al., *Phosphorylation and regulation of Akt/PKB by the rictor-mTOR complex.* Science, 2005. **307**(5712): p. 1098-101.
123. Garcia-Martinez, J.M. and D.R. Alessi, *mTOR complex 2 (mTORC2) controls hydrophobic motif phosphorylation and activation of serum- and glucocorticoid-induced protein kinase 1 (SGK1).* Biochem J, 2008. **416**(3): p. 375-85.
124. Saxton, R.A. and D.M. Sabatini, *mTOR Signaling in Growth, Metabolism, and Disease.* Cell, 2017. **168**(6): p. 960-976.
125. Marques-Ramos, A. and R. Cervantes, *Expression of mTOR in normal and pathological conditions.* Mol Cancer, 2023. **22**(1): p. 112.
126. Guri, Y. and M.N. Hall, *mTOR Signaling Confers Resistance to Targeted Cancer Drugs.* Trends Cancer, 2016. **2**(11): p. 688-697.
127. Fritsche, L., et al., *Insulin-induced serine phosphorylation of IRS-2 via ERK1/2 and mTOR: studies on the function of Ser675 and Ser907.* Am J Physiol Endocrinol Metab, 2011. **300**(5): p. E824-36.
128. Harrington, L.S., et al., *The TSC1-2 tumor suppressor controls insulin-PI3K signaling via regulation of IRS proteins.* J Cell Biol, 2004. **166**(2): p. 213-23.
129. Briaud, I., et al., *Insulin receptor substrate-2 proteasomal degradation mediated by a mammalian target of rapamycin (mTOR)-induced negative feedback down-regulates protein kinase B-mediated signaling pathway in beta-cells.* J Biol Chem, 2005. **280**(3): p. 2282-93.
130. Yu, Y., et al., *Phosphoproteomic analysis identifies Grb10 as an mTORC1 substrate that negatively regulates insulin signaling.* Science, 2011. **332**(6035): p. 1322-6.
131. Hsu, P.P., et al., *The mTOR-regulated phosphoproteome reveals a mechanism of mTORC1-mediated inhibition of growth factor signaling.* Science, 2011. **332**(6035): p. 1317-22.
132. Dibble, C.C., J.M. Asara, and B.D. Manning, *Characterization of Rictor phosphorylation sites reveals direct regulation of mTOR complex 2 by S6K1.* Mol Cell Biol, 2009. **29**(21): p. 5657-70.
133. Liu, P., et al., *Sin1 phosphorylation impairs mTORC2 complex integrity and inhibits downstream Akt signalling to suppress tumorigenesis.* Nat Cell Biol, 2013. **15**(11): p. 1340-50.

134. Battaglioni, S., et al., *mTOR substrate phosphorylation in growth control.* Cell, 2022. **185**(11): p. 1814-1836.
135. Huang, J., et al., *The TSC1-TSC2 complex is required for proper activation of mTOR complex 2.* Mol Cell Biol, 2008. **28**(12): p. 4104-15.
136. Lawrence, R.E., et al., *A nutrient-induced affinity switch controls mTORC1 activation by its Rag GTPase-Ragulator lysosomal scaffold.* Nat Cell Biol, 2018. **20**(9): p. 1052-1063.
137. Fernandes, S.A., et al., *Spatial and functional separation of mTORC1 signalling in response to different amino acid sources.* Nat Cell Biol, 2024. **26**(11): p. 1918-1933.
138. Napolitano, G., C. Di Malta, and A. Ballabio, *Non-canonical mTORC1 signaling at the lysosome.* Trends Cell Biol, 2022. **32**(11): p. 920-931.
139. Plas, D.R. and C.B. Thompson, *Akt activation promotes degradation of tuberin and FOXO3a via the proteasome.* J Biol Chem, 2003. **278**(14): p. 12361-6.
140. Alesi, N., et al., *TSC2 regulates lysosome biogenesis via a non-canonical RAGC and TFEB-dependent mechanism.* Nat Commun, 2021. **12**(1): p. 4245.
141. Asrani, K., et al., *An mTORC1-mediated negative feedback loop constrains amino acid-induced FLCN-Rag activation in renal cells with TSC2 loss.* Nat Commun, 2022. **13**(1): p. 6808.
142. Demetriades, C., M. Plescher, and A.A. Teleman, *Lysosomal recruitment of TSC2 is a universal response to cellular stress.* Nat Commun, 2016. **7**: p. 10662.
143. Prentzell, M.T., et al., *G3BPs tether the TSC complex to lysosomes and suppress mTORC1 signaling.* Cell, 2021. **184**(3): p. 655-674 e27.
144. Henske, E.P., et al., *Tuberous sclerosis complex.* Nat Rev Dis Primers, 2016. **2**: p. 16035.
145. Martin, K.R., et al., *The genomic landscape of tuberous sclerosis complex.* Nat Commun, 2017. **8**: p. 15816.
146. Astrinidis, A., et al., *Cell cycle-regulated phosphorylation of hamartin, the product of the tuberous sclerosis complex 1 gene, by cyclin-dependent kinase 1/cyclin B.* J Biol Chem, 2003. **278**(51): p. 51372-9.
147. Odle, R.I., et al., *An mTORC1-to-CDK1 Switch Maintains Autophagy Suppression during Mitosis.* Mol Cell, 2020. **77**(2): p. 228-240 e7.
148. Joshi, J.N., et al., *mTORC1 activity oscillates throughout the cell cycle, promoting mitotic entry and differentially influencing autophagy induction.* Cell Rep, 2024. **43**(8): p. 114543.
149. Hsieh, H.J., et al., *Systems biology approach reveals a link between mTORC1 and G2/M DNA damage checkpoint recovery.* Nat Commun, 2018. **9**(1): p. 3982.
150. Ebi, H., et al., *PI3K regulates MEK/ERK signaling in breast cancer via the Rac-GEF, P-Rex1.* Proc Natl Acad Sci U S A, 2013. **110**(52): p. 21124-9.
151. Vasan, N. and L.C. Cantley, *At a crossroads: how to translate the roles of PI3K in oncogenic and metabolic signalling into improvements in cancer therapy.* Nat Rev Clin Oncol, 2022. **19**(7): p. 471-485.
152. Elkabets, M., et al., *mTORC1 inhibition is required for sensitivity to PI3K p110alpha inhibitors in PIK3CA-mutant breast cancer.* Sci Transl Med, 2013. **5**(196): p. 196ra99.

153. Chapman, P.B., et al., *Improved survival with vemurafenib in melanoma with BRAF V600E mutation.* N Engl J Med, 2011. **364**(26): p. 2507-16.
154. Hauschild, A., et al., *Dabrafenib in BRAF-mutated metastatic melanoma: a multicentre, open-label, phase 3 randomised controlled trial.* Lancet, 2012. **380**(9839): p. 358-65.
155. Holderfield, M., et al., *Targeting RAF kinases for cancer therapy: BRAF-mutated melanoma and beyond.* Nat Rev Cancer, 2014. **14**(7): p. 455-67.
156. Salama, A.K. and K.T. Flaherty, *BRAF in melanoma: current strategies and future directions.* Clin Cancer Res, 2013. **19**(16): p. 4326-34.
157. Ilagan, E. and B.D. Manning, *Emerging role of mTOR in the response to cancer therapeutics.* Trends Cancer, 2016. **2**(5): p. 241-251.
158. Sharma, S.V., et al., *Epidermal growth factor receptor mutations in lung cancer.* Nat Rev Cancer, 2007. **7**(3): p. 169-81.
159. Tricker, E.M., et al., *Combined EGFR/MEK Inhibition Prevents the Emergence of Resistance in EGFR-Mutant Lung Cancer.* Cancer Discov, 2015. **5**(9): p. 960-971.
160. Pirazzoli, V., et al., *Acquired resistance of EGFR-mutant lung adenocarcinomas to afatinib plus cetuximab is associated with activation of mTORC1.* Cell Rep, 2014. **7**(4): p. 999-1008.
161. Gremke, N., et al., *mTOR-mediated cancer drug resistance suppresses autophagy and generates a druggable metabolic vulnerability.* Nat Commun, 2020. **11**(1): p. 4684.
162. Kowarz, E., D. Loscher, and R. Marschalek, *Optimized Sleeping Beauty transposons rapidly generate stable transgenic cell lines.* Biotechnol J, 2015. **10**(4): p. 647-53.
163. Nuchel, J., et al., *An mTORC1-GRASP55 signaling axis controls unconventional secretion to reshape the extracellular proteome upon stress.* Mol Cell, 2021. **81**(16): p. 3275-3293 e12.
164. Acharya, A. and C. Demetriades, *mTORC1 activity licenses its own release from the lysosomal surface.* Mol Cell, 2024. **84**(22): p. 4385-4400 e7.